EMEP Technical Report 2/2007
Date: July 2007

METEOROLOGISK INSTITUTT
Norwegian Meteorological Institute

First evaluation of the performance of the global EMEP model and comparison with the global OsloCTM2 model

Jan E. Jonson[1], Leonor Tarrasón[1], Peter Wind[1], Michael Gauss[1,2]
Semeena Valiyaveetil S.[1], Svetlana Tsyro[1], Heiko Klein[1], Ivar S.A Isaksen[2]
and Anna Benedictow[1]

[1] Norwegian Meteorological Institute
[2] Department of Geosciences, University of Oslo

EMEP MSC-W
Technical report 2/2007

ISSN 1504-6079 (print)
ISSN 1504-6206 (on-line)

Preface and Acknowledgments

This report has been prepared for presentation at the thirty-first session of the Steering Body to EMEP (Co-operative Programme for Monitoring and Evaluation of the Long Range Transmission of Air Pollutants in Europe). As a result of the development of the EMEP model in the past years to allow for a flexible choice of the model grid and domain, results from the global version of the model in longitude-latitude coordinates are presented here for the first time. The model results are compared here to measurements from several sources, including surface measurements from the EMEP, GAW (Global Atmospheric Watch) and EANET (Acid Deposition Monitoring Network in East Asia) databases, vertical sounding data from ozone sondes and remote sense data. In addition, as part of our on-going co-operation with the University of Oslo, Norway, the global EMEP model results are compared with their state-of art global model, OsloCTM2.

This work has received support from the Research Council of Norway through computer time granted at the Norwegian Metacenter for Computational Science (NOTUR). This work has been funded partly by the EMEP Trust Fund and partly by the Norwegian Ministry of the Environment.

Contents

CHAPTER 1

Introduction

The main reason to develop a global modelling system within EMEP is that many of the pollutants considered in the programme undergo significant intercontinental transport. The increased importance of intercontinental transport and the existence of significant pollution sources in areas susceptible for inter-hemispheric transport relevant to LRTAP advise the extension of hemispheric approaches to use global scale models instead.

An additional advantage of the global approach is that it will allow for a long-term stable development to support EECCA countries with information required for air quality control and help on the implementation of the protocols by Convention on Long-range Transboundary Air Pollution (LRTAP) in these countries.

To this purpose, a collaboration has been proposed this year for the modelling centers of EMEP (MSC-E and MSC-W). The aim of this collaboration is the gradual unification of their respective modelling systems to allow for the development of a common modular global system capable of operational computations of transboundary fluxes of acidifying pollutants, photo-oxidants, particulate matter, heavy metals and persistent organic compounds for all Parties to the LRTAP Convention.

The global model presented here would be a relevant first step for this co-operation. The development of the EMEP Unified model during the last few years has resulted in a flexible modelling system capable of bridging different scales, from local to regional, hemispheric and global. The EMEP Unified model is now flexible for use in different resolutions, and different grid projections for any given domain. This facilitates the interpretation of results in different scales and allows for a more transparent nesting system and treatment of boundary conditions.

Initially, the EMEP Unified model was developed at MSC-W in order to be run in finer resolution to address local scale air pollution problems (Wind et al. 2002, Slørdal et al. 2004). The development allowed also the extension of the EMEP domain

to hemispheric scale. Last year, the first results from the EMEP hemispheric model were presented in Jonson et al. (2006). The natural next step was the realization of an application in global scale, showing the capability of the model with different choice of grid projection.

The main difference between the hemispheric and the global EMEP model versions is the choice of grid projection and the extension of the domain. The global EMEP model uses a latitude longitude projection with a 1°x 1° resolution, whereas the hemispheric model uses a polar stereographic projection with 100 x 100km^2 resolution. In addition model results in the global model version are not constrained by lateral boundary concentrations since it has global coverage. Apart from that, model formulations are virtually identical, also with respect to the regional and local versions of the EMEP model. Consequently, we expect that the global EMEP model version performs very similarly to the hemispheric EMEP model version.

This report documents the performance of the global version of the EMEP Unified model versus observations and compares its performance with that of the global OsloCTM2 model. It is part of the consolidated co-operation with the University of Oslo, initiated last year to provide better insight in different approaches to study intercontinental pollution transport.

Both the EMEP hemispheric model and the OsloCTM2 model have participated in the TF HTAP (Task Force on Hemispheric Transport of Air Pollution) Coordinated Model Inter-comparison Studies (http://aqm.jrc.it/HTAP/). Model results and source-receptor relationships for intercontinental transport have been calculated by about 30 different models for a large number of air pollutants and results from this inter-comparison is currently under evaluation.

A large amount of data has been generated by the global EMEP and OsloCTM2 models for this report, including hourly 3-D fields of ozone and nitrogen dioxide (NO_2), 2-D surface fields of maximum and daily mean values, vertical profiles of ozone, nitrogen monoxide (NO), NO_2, carbon monoxide (CO), sulphur dioxide (SO_2) and sulphate (SO_4) at selected stations, emission data sets, etc. This report shows first comparisons based on these new data. It is expected that the results will help understanding the performance of the models also in the HTAP inter-comparison. Further analysis will be done, also with the help of the HTAP inter-comparison project and its visualization tools, to better understand the differences between the two models and to identify ways of improving their ability to reproduce measurements.

CHAPTER 2

Models and methodology used

Short descriptions of the two global models, the EMEP global model and the global OsloCTM2 model, are given below together with a description of the model runs setup for comparison with observations.

2.1 The global EMEP model

The EMEP Unified model is a multi-layer atmospheric dispersion model designed for simulating the long-range transport of air pollution over several years. The EMEP model is flexible with respect to the choice of horizontal grid projection, domain and resolution. It can be run at local, regional, hemispheric and global scale.

The global version of the EMEP model has 20 vertical layers in sigma-coordinates up to 100hPa, the same as in the regional version of the model. The horizontal grid is regularly spaced latitude/longitude with 1° x 1° resolution. To allow for global model applications, the EMEP model code has been revised to allow flexible choice of grid projection. In addition, some modifications had to be introduced in the EMEP model in order to treat efficiently the singularity at the poles in a latitude/longitude grid projection. The result is a common EMEP model code for all scale applications. The global EMEP model differs from the regional model only by the input data used to drive the model, namely meteorology, emissions and description of land cover.

For the results shown in this report, the EMEP model version rv2_7_2 has been used. As in the regional model, the numerical solution of the advection terms is based upon the scheme of Bott (1989). The fourth order scheme is utilized in the horizontal directions. In the vertical direction a second order version applicable to variable grid distances is employed. The chemical scheme uses about 140 reactions between 70 species and couples the sulfur and photochemistry. The partitioning between ammonia,

nitric acid and the inorganic aerosol components is calculated by using the EQSAM module Metzger et al. (2002a,b). The dry deposition module is based on the resistance analogy and is calculated independently over 17 different land-use types. Inside the EMEP area, EMEP land-use data is used in the global version. Outside the EMEP area land-use data from MM5 is used. The surface resistance is the most complex variable in the deposition model, ans it is parametrized for the different components as described in Simpson et al. (2003) and according to Nemitz et al. (2001) and Fowler and Erisman (2003). Parametrization of the wet deposition processes in the EMEP model includes both in-cloud and sub-cloud scavenging of gases and particles, using scavenging coefficients. The model is documented in detail in Simpson et al. (2003).

Compared to the OsloCTM2, the EMEP global model can be run very fast. It requires only 8 hours for a full year global simulation, using 48 processors.

2.2 The OsloCTM2 model

The OsloCTM2 is a global 3D chemical transport model driven by ECMWF meteorological data extending from the ground to 10 hPa in 40 vertical layers, or up to 0.1 hPa in 60 vertical layers. Also for the horizontal resolution several options are available. In the studies for this report we have chosen the 40-layer version with Gaussian T42 (about 2.8° x 2.8°) and regular 1° x 1° resolutions. Advection uses the Second Order Moment scheme of Prather (1986), while convection is based on the Tiedtke (1989) mass flux scheme. Transport in the boundary layer is treated according to the Holtslag K-profile method (Holtslag et al. 1990), and the calculation of dry deposition follows Wesely (1989). Surface emissions including also biogenic NMVOC emissions are based on GEIA (http://www.geiacenter.org), the EDGAR v3.2 data base (Olivier and Berdowski 2001), the POET project (Olivier et al. 2003), and the RETRO project (http://retro.enes.org/), and are typical of the year 2001. Lightning emissions of NOx are parametrized based on formulas by Price et al. (1997a) and Price et al. (1997b), distributing the emissions according to convective activity in the model and choosing 5 Tg(N)/year as total annual output. The model calculates the distribution of 105 chemical compounds through comprehensive modules for tropospheric chemistry (Berntsen and Isaksen 1997, 1999, Berglen et al. 2004) and stratospheric chemistry (Stordal et al. 1985, Isaksen et al. 1990). Photo-dissociation rates are calculated on-line by the Fast-J module (Wild et al. 2000), taking into account changing ozone distributions and the scattering of sunlight by clouds.

2.3 Experiment setup

Since the purpose of this report is to characterize the performance of these two global models against observations, long-term calculations covering the whole year of 2001, with hourly and daily resolution have been carried out. In order to understand better

the origin of differences between the two models, the model simulations for 2001 were designed to be as similar as possible, based on common meteorological input and similar set of emission input data. It was initially envisaged to use also simulations with the same horizontal resolution, but this was not possible due to CPU limitations for the OsloCTM2 runs. Therefore, the global version of the EMEP model has been run with 1° x 1° resolution while the OsloCTM2 model has been run on T42 resolution (about 2.8° x 2.8°) for the whole of 2001. In addition, the OsloCTM2 model has been run then with 1° x 1° resolution for selected short periods in January 2001 and July 2001.

2.3.1 Meteorological input

The meteorological data used here have been prepared by running the Integrated Forecast System model (IFS) of ECMWF for the year 2001 at a spectral resolution of T319. For the model runs in this study the data have been truncated to Gaussian T42 (about 2.8° x 2.8°) and to a regular 1° x 1° grid.

The source of the meteorological data used by the global EMEP model is the same as in the OsloCTM2 model (1° x 1° grid, see below). Since the EMEP model is not yet flexible in the choice of vertical coordinates, the vertical levels had to be interpolated from originally 40 hybrid levels into 20 sigma levels. The vertical velocities in sigma coordinates have been derived from the original pressure derivatives, and the resulting winds filtered in both vertical and horizontal directions, in order to obtain divergence free wind fields.

For the OsloCTM2 model runs, the initialization for the model runs was taken from a previous T42 model run using year 1999 and 2000 data. The model was thus effectively spun up for more than one year. For most results in this report, one T42 run covering the entire year of 2001 was used. This run created restart files at selected dates of the year, from which short-term continuation runs were performed in 1° x 1° resolution. T42 restart files contain the entire set of second order moments and have thus an effective resolution about three times better than T42. This advantage was fully exploited when the 1° x 1° runs were started. Due to the high CPU time requirement of OsloCTM2, which primarily derives from the use of the highly accurate Second Order Moment scheme (Prather 1986), the 1° x 1° runs could not be integrated for more than two 2-week periods for this report. While it is realized that the high CPU time requirement hampers long-term integrations with the OsloCTM2 in this high resolution at this point, we do believe that, with increasing computer power, this finer resolution model version will become increasingly useful in the years to come.

2.3.2 Emission input

The global emissions used by OsloCTM2 model are described above (section 2.2).

For the global EMEP model runs, the emissions used are a compilation from different sources. This is far from an optimal set of emissions, but these are the result of

testing with the global EMEP model different available emission sets. Such tests have been facilitated by the effective use of CPU resources in the global EMEP model.

In the Southern Hemisphere and over North America, the global emissions have been adapted from the OsloCTM2 emission input and converted into SNAP Level 1 emission codes. In the EMEP area, EMEP emissions are used, to secure that the results from the global model over Europe is as similar as possible to the results from the regional EMEP model. Over Asia, the OsloCTM2 emissions have been replaced by a bottom up inventory developed for East Asia for the year 2000 (Streets et al. 2003) available through ACESS (Ace-Asia and Trace-P Modeling and Emission Support System) at http://www.cgrer.uiowa.edu/ACESS/acess_index.htm

For biogenic VOC emissions, the OsloCTM2 model uses prescribed values. In the global EMEP model, temperature dependent biogenic VOC emissions from forests are used instead, following the methodology of the EMEP regional model. In particular for ozone formation, the natural NMVOC emissions are very important. In the regional version of the EMEP model natural NMVOC emissions are calculated based on tree species, near surface temperature and a crude formulation for global radiation as described in Simpson et al. (1995). Applying these calculated natural NMVOC emissions rather than the NMVOC emissions described in section 2.2 has a marked effect on the model results as further described in Chapter 3.

The EMEP model makes use of yearly gridded emissions for different emission sectors. For each country and sector, the model uses time factors that determine the daily, weekly and monthly variations. For the global model application in this report, we have used OsloCTM2 monthly emissions coupled with daily variations outside the EMEP area. Inside the EMEP area, the EMEP temporal emission variations are used.

Volcanic emissions of sulphur are included only within the EMEP domain. No natural DMS emissions are included in the global EMEP model calculation.

CHAPTER 3

Main differences in global emission input

The results from the two global chemical transport models, the EMEP global and the OsloCTM2 models, will be driven to a large extent by their input emission values. An overview of the main differences in the global emissions used by the two models is given below.

Differences between the emissions used by the two global models are significant for all components, also for natural emissions. In Table 3.1 the global anthropogenic emission totals used by the two different models are presented. For the 1° x 1° grid calculations with the OsloCTM2 model, the total emissions are the same as in Table 3.1. Emissions in the T42 runs are just aggregated from the 1° x 1° runs. It is relevant to note that the NOx emissions are significantly lower in the global EMEP model input while SOx emissions are larger than those used by the OsloCTM2 model.

In the Southern Hemisphere and over North America, emissions are the same in both models. The main differences are thus located over Europe and Asia. Figure 3.1 show the position and extent of the main differences in emissions of nitrogen oxides, sulphur dioxide and ethane over Europe and Asia.

NOx emissions are lower in the global EMEP model input both over Europe and Asia. Specially in China, the ACESS data is much lower that the GEIA data used by the OsloCTM2 for the area. For SOx emissions, the EMEP emissions over Europe are lower than the RETRO data used by the OsloCTM2 model. Over Asia, SOx emissions in the ACESS data are higher than the GEIA data. This seems to be related to the trend evolution of the sulphur emissions. For sulphur emissions, there is a decreasing trend over Europe (Vestreng et al. 2007), whereas emissions have been increasing in Asia, suggesting that the OsloCTM2 input emissions are more representative for an earlier year than 2001. Anthropogenic Non Methane Volatile Organic Carbon (NMVOC) emissions are in general higher in Europe and Asia in the emissions used by the EMEP global model. However, as indicated in the scales of Figure 3.1, differ-

ences in anthropogenic VOC emissions are small. The most significant difference is for natural emissions of hydrocarbons, in particular isoprene, as further discussed in section 3.2.

Table 3.1: Total anthropogenic global emissions used in this report (Tg $yr^{-}1$)

Component	EMEP_Global	OSLO_CTM2
CO (as CO)	829	964
NOx (as NO_2)	102	124
NH3 (as NH_3)	52	46
SO2 (as SO_2)	65	56
NMVOC (as NMVOC)	103	80

3.1 NO_2

Although it is difficult to validate emissions of nitrogen dioxide, we have made an attempt to compare the model results of the NO_2 tropospheric column with measurements derived from the GOME satellite. The NO_2 column is determined by the source strength, chemical loss and deposition and advection. As the lifetime of NO_2 is very short, ranging from a few days in the winter to a few hours only in summer, NO_2 is in general not advected far from its sources. Thus the NO_2 column can be used to locate source regions, and also as a relative good measure of the source strength.

In Figures 3.2 and 3.3 the monthly averaged model calculated NO_2 column is shown along with the NO_2 column as measured by the GOME satellite respectively for January and July 2001. The main source regions can be identified in both the measured and model calculated columns. The high columns calculated by both models over Australia are not seen in the satellite data. A possible explanation is that the estimated emissions from Australia may be too strong, however such possibility needs to be further analyzed with the help of ground measurements over Australia. Both in January and in July, over China, the EMEP global model using ACESS emission data calculates lower columns than those derived from satellite measurements. A possible explanation for this is that emissions are underestimated in this region. This would be in agreement with the conclusions from Wang et al. (2007), using NO_2 columns from the GOME satellite to constrain NOx emissions. They estimated that Chinese emissions are underestimated by 33% in the GEIA data sets (Benkovitz et al. 1996), and as indicated in Figure 3.1, the GEIA data set used by OsloCTM2 has somewhat higher emissions than the ACESS data used by the global EMEP model. Therefore

the underestimation of emissions with EMEP can be larger than in OsloCTM2 model results. According to Wang et al. (2007) there should be a ratio of 1.4 between winter and summer emissions. As we assume constant emissions throughout the year in this region, most of the underestimation should be attributed to the winter months. The OsloCTM2 underestimation is somewhat less pronounced over China than for the EMEP model, consistent with the fact that their input NOx emissions are higher than those used by the EMEP global model.

However, it is difficult to conclude on the quality of emission data just from the performance of the two models versus column observations derived from satellites, independently of the recognized caveats of the measurement data. Over North America, where the emissions used by both models are the same, OsloCTM2 shows generally higher NO_2 columns than the EMEP model. Also over Europe, where the emissions from RETRO used by the OsloCTM2 model are lower than the EMEP emissions, the OsloCTM2 model derives higher NO_2 column values. There is a systematic behavior in the OsloCTM2 model that results in generally higher NO_2 column values than in the global EMEP model. The reasons for this behavior are not clear but they can be dependent on different parametrizations of lightning emissions in the free troposphere (a small effect), different chemical schemes and/or differences in the treatment of dry and wet deposition.

3.2 Isoprene emissions and formaldehyde

Another significant difference in the input values used by the two global models concerns the biogenic isoprene emissions. Unfortunately, isoprene emissions are not directly comparable with observations from satellites, but a good marker for isoprene emissions is the concentration of formaldehyde (HCHO), even though emissions of other NMVOC will also produce formaldehyde.

A comparison of formaldehyde columns from the EMEP hemispheric model results and observations derived from the GOME satellite was already presented in Jonson et al. (2006). The comparison showed a general good agreement over Europe, North America, India and China between the EMEP model estimates and the values derived from GOME.

The results from OsloCTM2model, using prescribed isoprene emissions are generally considerably lower than the global EMEP model results using isoprene emissions calculated as described in section 2.3.2. In Figure 3.4 the difference between the total formaldehyde column derived from the EMEP global model and the values calculated by the OsloCTM2 model are presented. In most areas the column values calculated with the global EMEP model are larger. In particular over North America where other anthropogenic NMVOC emissions are the same, the larger EMEP global model results seem to confirm the relevance of the calculation of isoprene emissions in the total column concentrations of formaldehyde.

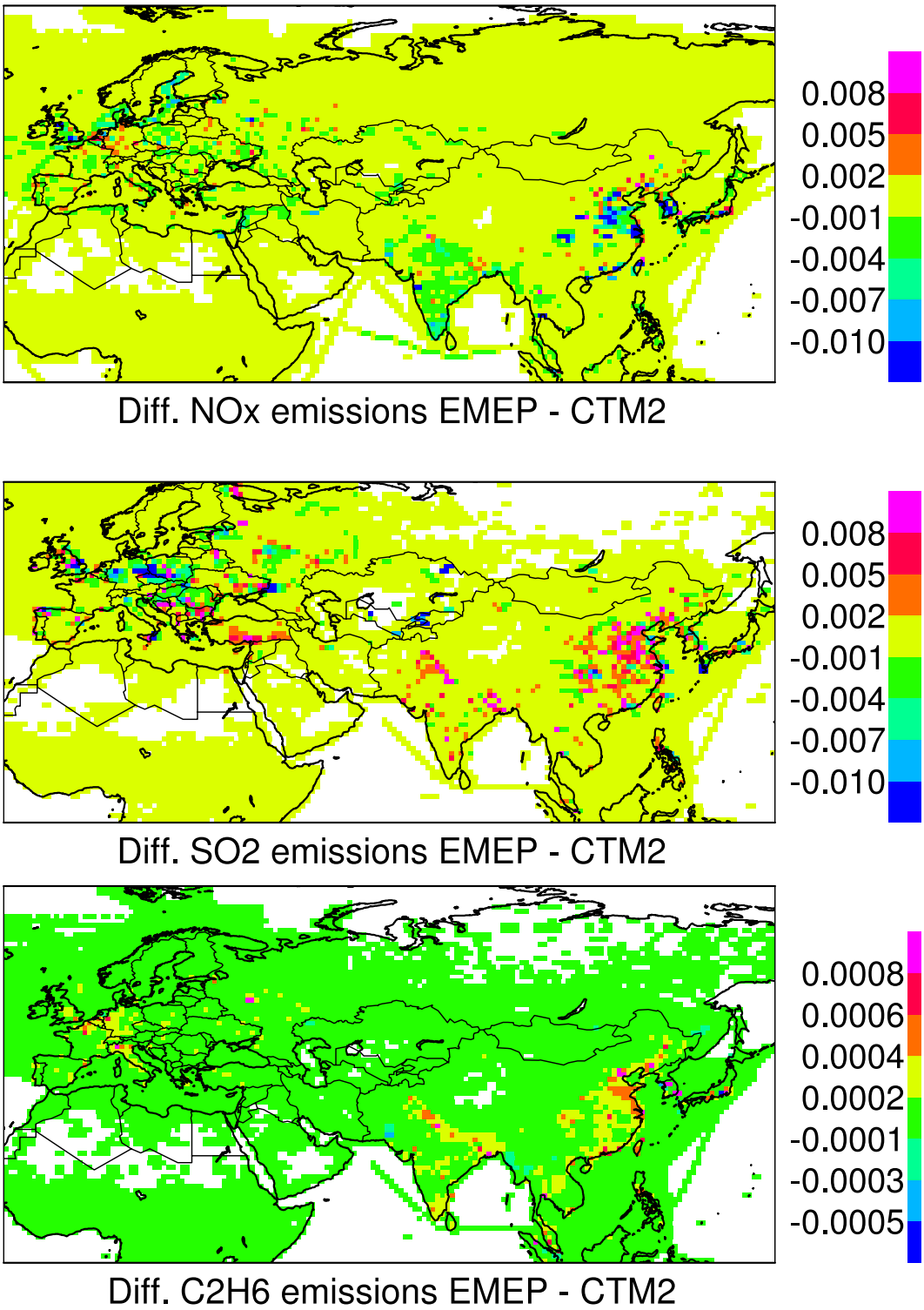

Figure 3.1: Difference in emission values over Europe and Asia between the EMEP model input and the OsloCTM2 model input. Differences in NOx emissions in $Gg(NO_2)$/year are in the top panel, SO_2 emissions in $Gg(SO_2)$/year in the middle panel and ethane (C_2H_6) emissions in Gg(NMVOC)/year in the bottom panel.

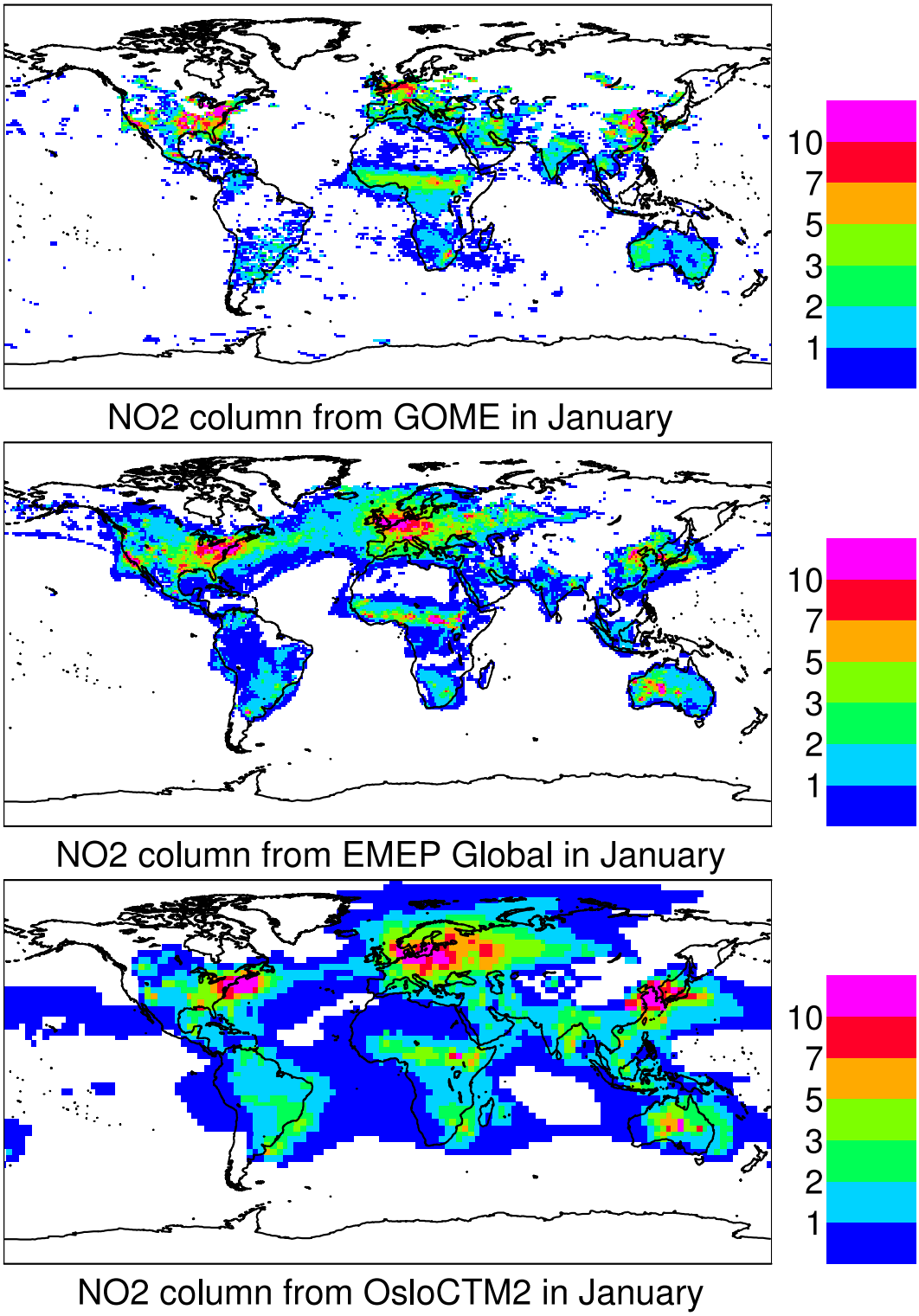

Figure 3.2: January NO_2 column (10^{15} molecules cm^{-2}) from GOME (top) and calculated with the EMEP global and OsloCTM2 models.

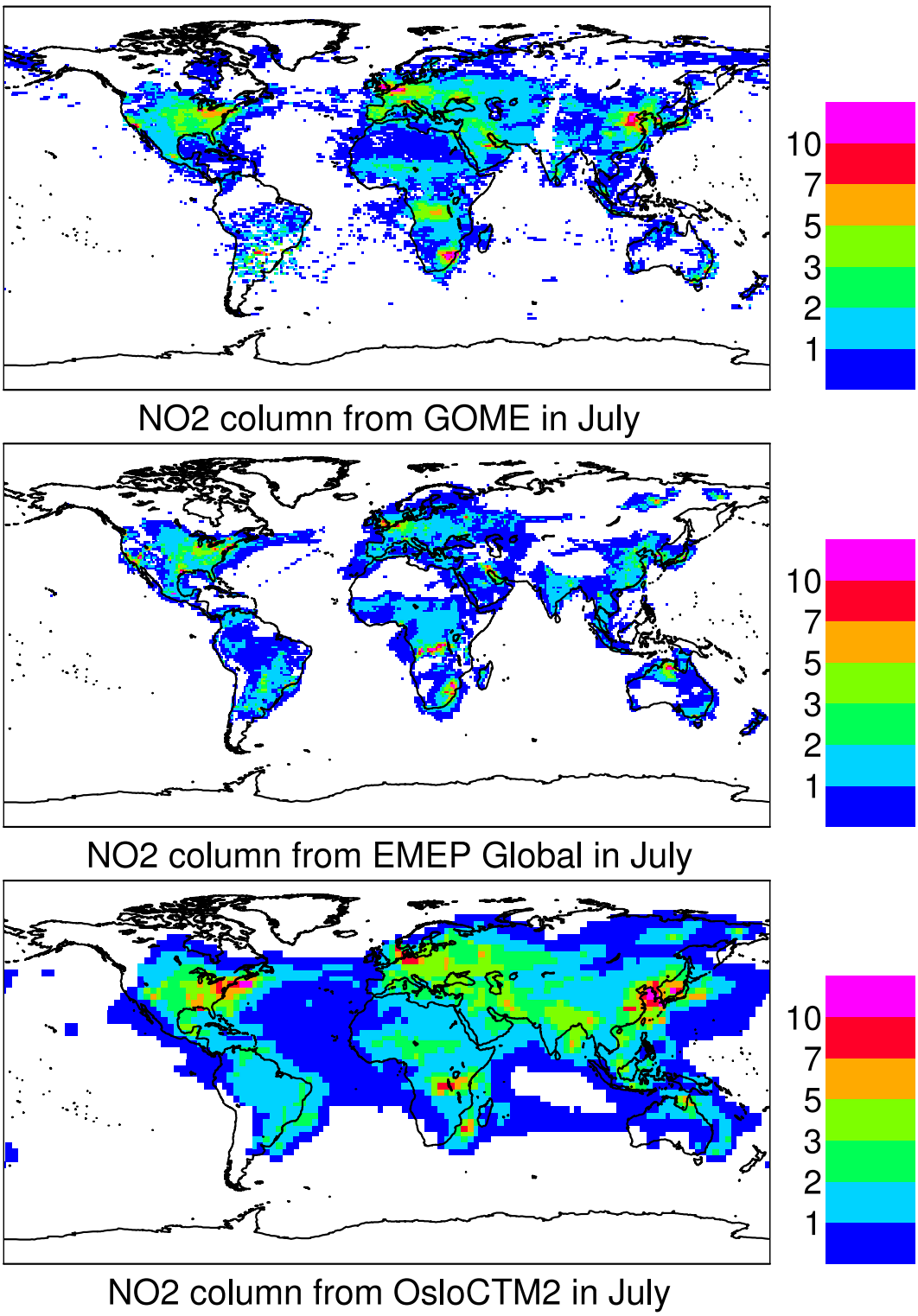

Figure 3.3: July NO_2 column (10^{15} molecules cm^{-2}) from GOME (top) and calculated with the EMEP global and OsloCTM2 models.

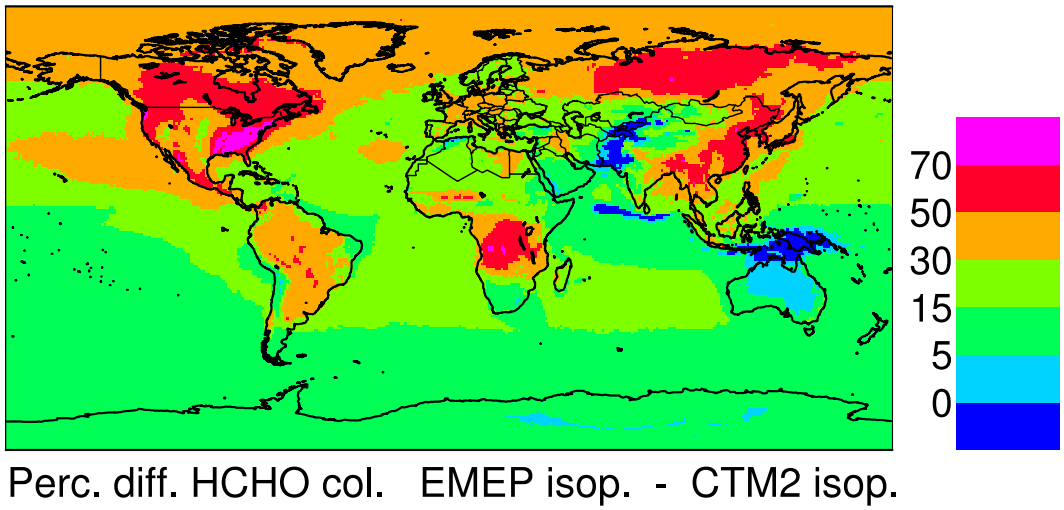

Figure 3.4: Percentage difference in annual total HCHO column with isoprene calculated as in the EMEP model − isoprene emissions as in the OsloCTM2 model. Units: (%).

CHAPTER 4

Comparison of model results with measurements

The measurement data used for evaluation of the model performance are those available through the EMEP, http://www.nilu.no/projects/ccc/index.html, GAW (Global Atmospheric Watch, http://gaw.kishou.go.jp/) and EANET (Acid Deposition Monitoring Network in East Asia) networks.

Most of the model evaluation below for OsloCTM2 is done for calculations with coarse resolution (T42 calculations). The OsloCTM2 has also been run with a 1° x 1° resolution for two short periods in January and July 2001. Some results from this finer resolution model run are shown in section 4.1.4 below in order to identify the effect of resolution in the OsloCTM2 model calculations. For the global EMEP model, the resolution of the evaluated results is 1° x 1°.

4.1 Surface measurements

4.1.1 Ozone

Ozone calculated with both models is shown for a selection of sites in Figure 4.1 and Figure 4.2. In addition, annual means of ozone daily maximum values and temporal correlations are listed for a large number of sites in Table 4.1.

For surface ozone, the two global models show very similar performance. For both models, the performance over Europe is generally better than for other regions, as shown in Figure 4.1. This is likely because the input data and to a certain extent also the measurements available for this report have higher quality over Europe than in other studied areas.

The OsloCTM2 model appears to perform better in mountainous regions such as the Alps, whereas the EMEP global model appears to perform better in western Eu-

rope, most likely associated to the model use of better emission data in the European region.

The performance of the global EMEP model is very similar over Europe to the performance of the regional EMEP model. Differences in model performance between the regional and the global model are only due to differences in the resolution and accuracy of the meteorological input data. As indicated in Jonson et al. (2006) and visualized in Figure 4.2, the EMEP global performance is worse over stations affected by deep convection, such as in Cape Matatula (S514). This is probably due to the simplified parametrization of convection in the EMEP model. Further model development is presently addressing this issue, as explained in Chapter 5.

The OsloCTM2 model has problems with large underestimations in polar regions, in contrast with a general overestimation of surface ozone levels close to source regions, see Figure 4.2. It is not clear yet what are the reasons for such underestimation but they may be related to the parametrization of dry deposition of ozone over snow surfaces.

Table 4.1: Comparison of Modeled versus Observed ozone for year 2001. Concentrations are 12-monthly Means of Daily Maximum Ozone Values. Correlation coefficients (r) are also between daily max values.

Code	Station	Obs.	EMEP_global		OsloCTM2	
		(ppb)	(ppb)	r	(ppb)	r
	Nordic Countries					
DK05	Keldsnor	35.49	36.18	0.696	40.83	0.71
DK31	Ulborg	37.22	38.15	0.684	38.73	0.57
FI09	Utoe	41.64	40.16	0.683	34.51	0.52
FI17	Virolahti II	38.01	31.91	0.746	26.84	0.47
NO01	Birkenes	36.53	36.15	0.510	38.40	0.36
NO45	Jeløya	35.88	33.94	0.703	37.43	0.69
NO48	Voss	36.98	36.02	0.423	38.66	0.39
NO42	Spitzbergen	37.94	34.47	0.373	25.05	0.41
SE02	Rørvik	38.81	35.42	0.719	35.53	0.48
SE11	Vavihill	38.55	35.85	0.744	39.57	0.74
SE35	Vindeln	36.18	30.61	0.617	33.49	0.55
	E European Countries					
EE09	Lahemaa	41.02	33.65	0.663	33.98	0.47
LT15	Preila	38.13	37.00	0.703	40.52	0.75
CZ01	Svratouch	40.68	38.16	0.752	44.31	0.75
CZ03	Kosetice	40.12	38.28	0.725	44.35	0.77
HU02	K-pusta	46.63	40.82	0.774	45.48	0.81

continued on next page

Code	Station	Obs.	EMEP_global		OsloCTM2	
PL02	Jarczew	39.33	37.08	0.749	41.93	0.77
PL04	Leba	41.16	36.13	0.719	40.75	0.75
RU16	Shepeljovo	36.28	32.90	0.735	28.98	0.57
SK06	Starina	43.49	38.53	0.640	44.12	0.68
SI08	Iskraba	49.45	44.33	0.798	47.43	079
SI31	Zarodnje	46.58	42.04	0.815	46.64	0.83
SI33	Kovk	44.86	42.15	0.827	46.80	0.82
C and NW European Countries						
AT02	Illmitz	43.46	40.55	0.804	44.51	0.82
CH02	Payerne	41.85	42.93	0.738	45.38	0.82
CH03	Taenikon	41.22	43.31	0.713	44.58	0.77
DE01	Westerland	40.43	39.68	0.744	40.00	0.68
DE02	Waldhof	38.20	35.58	0.811	43.26	0.78
DE03	Schauinsland	49.22	42.19	0.784	44.68	0.75
DE09	Zingst	37.75	37.01	0.680	36.47	0.59
FR08	Donon	46.75	39.64	0.850	44.56	0.80
FR09	Revin	39.81	38.76	0.775	43.97	0.76
FR10	Morvan	38.23	39.71	0.787	44.73	0.78
FR12	Iraty	50.09	40.95	0.738	45.33	0.68
IE31	Mace Head	39.22	38.65	0.577	39.65	0.53
GB02	Eskdalemuir	31.54	35.17	0.669	38.97	0.68
GB13	Yarner Wood	37.92	38.54	0.678	41.60	0.69
GB33	Bush	35.06	35.19	0.612	38.45	0.63
GB39	Sibton	34.68	35.69	0.753	39.11	0.57
BE01	Offfnage	39.76	38.73	0.765	44.23	0.75
NL10	Vreedepeel	34.56	33.70	0.820	44.99	0.77
Mediterranean Countries						
ES07	Viznar	48.42	43.91	0.822	48.37	0.81
ES08	Niembro	35.74	42.09	0.628	44.98	0.67
ES12	Zarra	48.94	44.96	0.857	46.78	0.82
ES14	Els Torms	44.20	43.60	0.814	46.71	0.76
IT01	Montelibretti	53.40	46.13	0.771	52.31	0.85
IT04	Ispra	46.64	47.78	0.831	48.36	0.75
MT01	Giordan Lighthouse	58.51	46.82	0.691		
GR02	Finakalia	51.22	47.33	0.743	52.12	0.81
GAW region 1 (Africa)						
A123	Assekram (Algerie)	36.35	36.18	0.50	37.70	0.48
C134	Cape Point (S. Africa)	25.11	30.64	0.64	26.09	0.36
I128	Izana (Canary Isl.)	46.31	35.20	0.23	42.02	0.32
GAW region 2 (Asia)						
M224	Minamitorishima (Japan)	28.03	18.35	0.84	28.45	0.87
Y224	Yonagunijima (Japan)	39.16	33.90	0.68	43.42	0.77
T236	Tsukuba (Japan)	22.67	23.70	0.36	48.49	0.51

continued on next page

Code	Station	Obs.	EMEP_global		OsloCTM2	
R239	Ryori (Japan)	35.58	32.31	0.62	42.93	0.17
GAW region 3 (S. America)						
U354	Ushuaia (Argentina)	18.35	20.13	0.79	18.46	0.53
GAW region 4 (N. America)						
S448	Saturna (Canada)	27.31	28.14	0.49	28.63	0.61
K444	Kejimkujik (Canada)	34.70	36.14	0.50	40.20	0.42
E449	Experimental Lakes (Ca.)	31.92	27.03	0.44	25.13	0.35
E444	Egbert (Canada)	31.98	34.97	0.63	29.53	0.60
B450	Bratt's Lake (Canada)	28.60	23.10	0.47	23.41	0.53
GAW region 5 (Pacific)						
T504	Tanah Rata (Malaysia)	20.13	28.14	-0.07	36.36	0.26
S514	Cape Matatula (Samoa U.S)	14.41	17.32	0.82	17.92	0.82
M519	Mauna Loa (U.S)	38.36	29.82	0.44	29.60	0.50
C540	Cape Grim (Australia)	25.58	28.64	0.63	23.60	0.37
GAW region 7 (Antarctica)						
S769	Syowa Station	24.87	28.74	0.91	14.00	0.48
M777	McMurdo/Arrival Height	25.00	26.95	0.93	14.64	0.45

4.1.2 Carbon monoxide

In Figure 4.3 model calculations are compared to measurements. CO measurements for a few sites are available on a hourly basis through the GAW website but such measurements are not available from the EMEP network. This is therefore the first time that CO comparison with observations is presented for the EMEP model. The two global models have a fairly similar performance versus observations.

It is however surprising that the two models perform better in the Japanese stations (Ryori, Minamitorishima and Yonagunijima) than they do in some European stations. In particular, the two models greatly underestimate measured CO at three European sites (Hohenpeissenberg, Kosetice and Kollumerwaard). For Hohenpeissenberg, this can be related to the fact that this is a mountain site, but it is difficult to understand why both models underestimate CO at Kosetice (CZ) and Kollumerwaard (NL). It may be related to accuracy of CO emissions. Since CO has a long lifetime, its concentration in the atmosphere is expected to be well mixed so that high peak levels in the measurements would primarily indicate the influence of nearby sources. It can be mentioned that the CO/NOx ratio for traffic emissions in the Czech Republic and in The Netherlands is somewhat lower than for other European countries (Vestreng, pers.comm.). However, and without any further evaluation of the quality of the measurement data at Kosetice and Kollumerwaad, it is difficult to conclude whether the emissions from CO used in this study are correct or not.

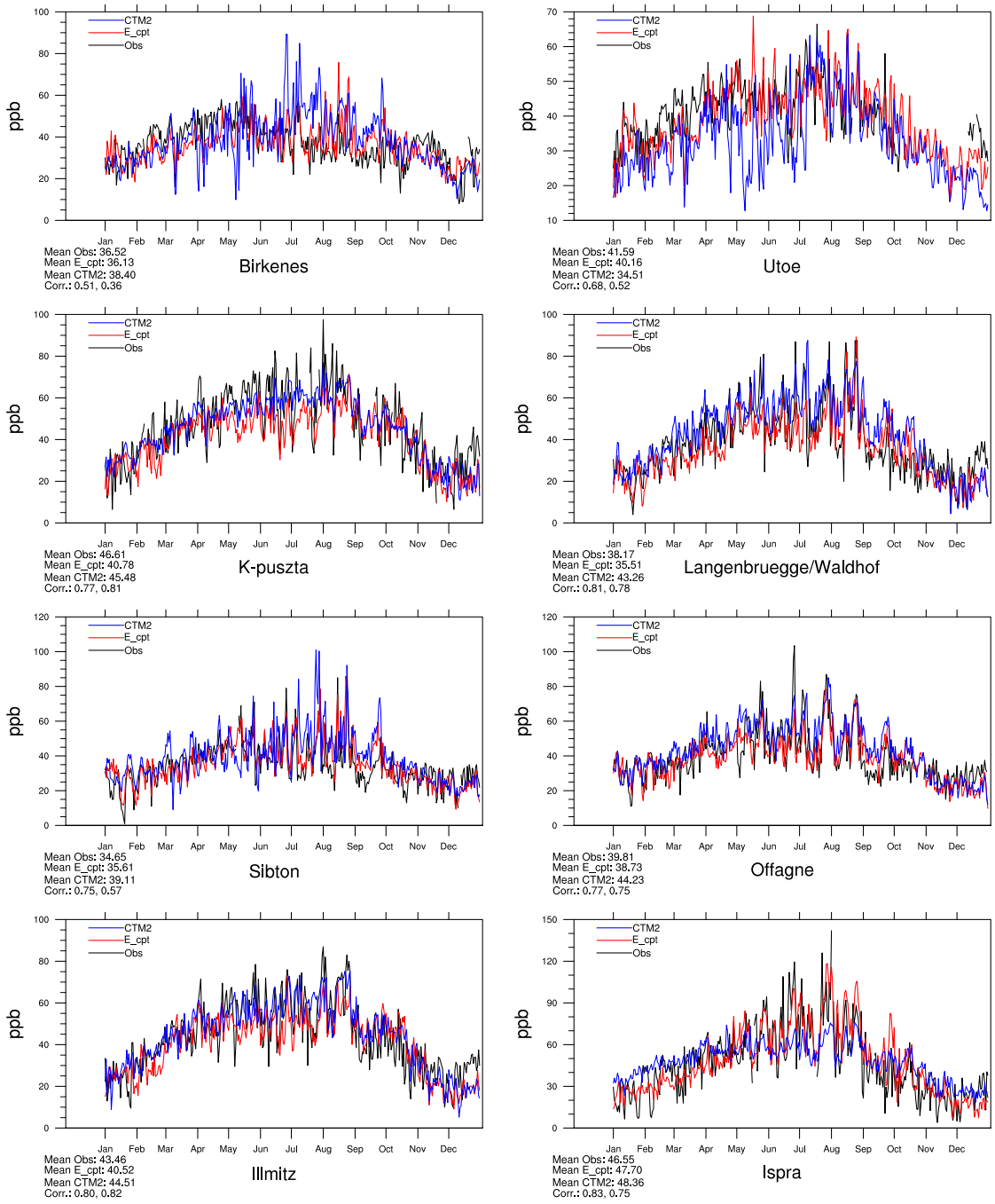

Figure 4.1: Modeled versus Observed Daily Maximun Ozone (ppb) for selected European stations in 2001. Observations are in black, global EMEP model results in red and OsloCTM2 model results in blue.

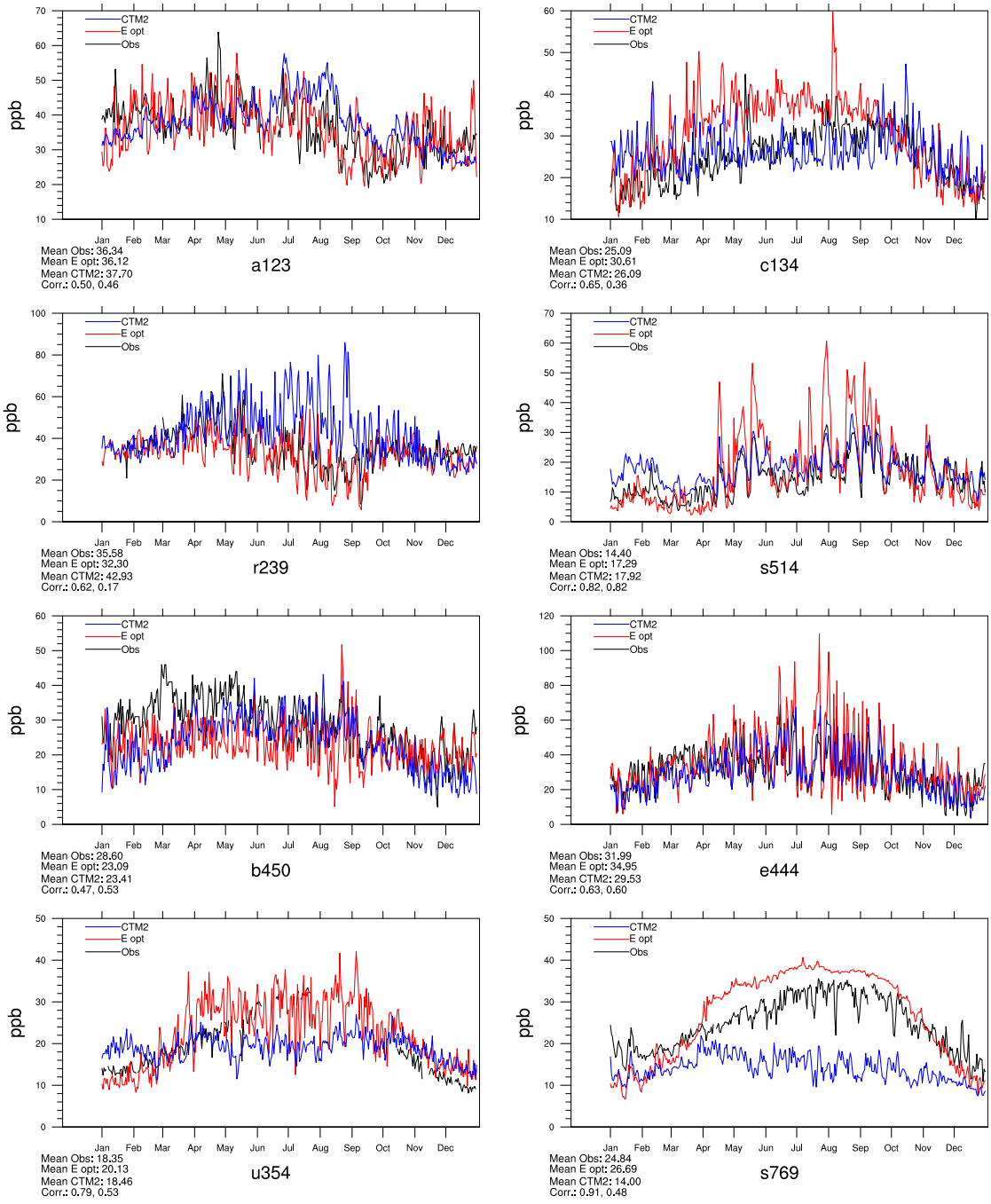

Figure 4.2: Modeled versus Observed Daily Max Ozone (ppb) for selected GAW stations in 2001. Observations are in black, global EMEP model results in red and OsloCTM2 model results in blue. Station names are according to Table 4.1.

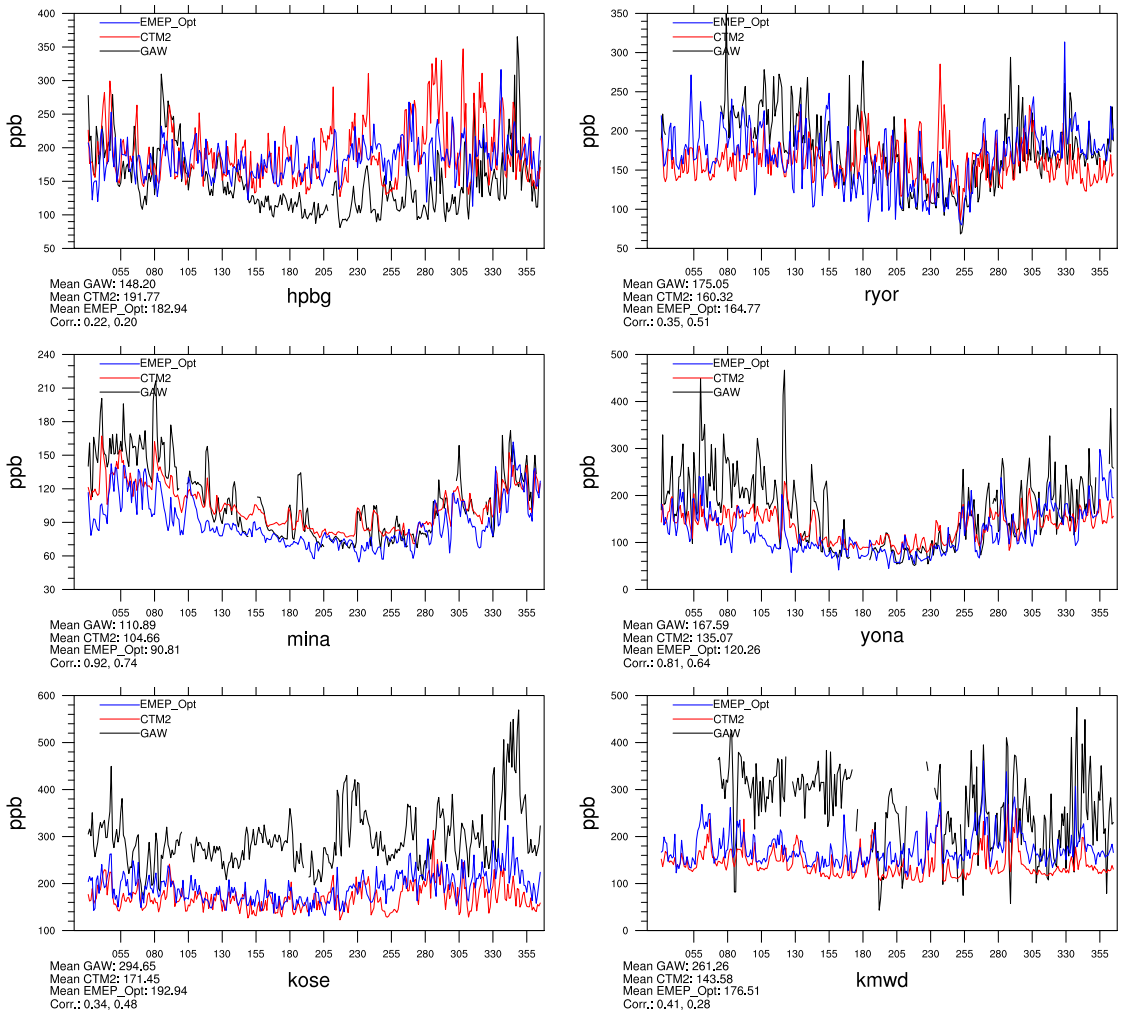

Figure 4.3: Modeled versus Observed Daily mean CO (ppb) at different GAW stationsin 2001. Observations are in black, global EMEP model results in blue and OsloCTM2 model results in red.

4.1.3 Sulphur species

In Figure 4.4 annual scatter plots for sulphur dioxide (SO_2), sulphate SO_4 in air over Europe are shown for both the OsloCTM2 and the EMEP global model. In the lower panels, precipitation values and wet deposition values from the EMEP global model are also compared with EMEP observations. These species have typical lifetimes of a few days, and therefore the variability of the concentrations within the geographical area covered by the models is substantial. The somewhat better correlation in the EMEP model is probably related to higher grid resolution and to some extent also to the use of more accurate emissions in Europe. The model results from the EMEP

global model version are very similar to the results from the hemispheric version as presented in Jonson et al. (2006).

Table 4.2: Comparison of Modeled versus Observed SO_2 for Year 2001 in EANET stations. Concentrations are 12-monthly means of daily values.

Station	Obs.	EMEP_global		OsloCTM2	
SO_2	μg(S)m^{-3}	μg(S)m^{-3}	r	μg(S)m^{-3}	r
Xian (Xiangzhou)	9.67	2.03	0.50	2.35	0.66
Jinyunshan	9.66	6.67	0.19	23.76	0.40
Weishuiyuan	4.85	10.16	0.05	12.65	0.01
Banryu (Japan)	0.98	0.75	0.02	2.25	0.17

Time series of sulphur dioxide concentrations calculated by the two global models are compared to observations over a selection of European EMEP stations in Figure 4.5.

The first row shows the performance of the global models at two mountain stations. Both models overestimate SO_2 at these stations at most times of the year, but the overestimation by the OsloCTM2 is much larger, in the case of Chopok (CZ) almost by a factor of 8. The discrepancies between the measurements and model simulations at these mountain stations are not easily explainable. Considering the location of these background measurement stations, one can expect that grid models with resolution of 50x50 km^2 and coarser will usually overestimate the measurements of SO_2 concentrations in mountain stations. Also it is important to reconsider whether it makes sense to compare the model surface concentrations with them, because in most cases the surface of those stations lie on the 3^{rd}, 4^{th} or 5^{th} level of the model. Still, the OsloCTM2 tendency to overestimate surface concentrations of SO_2 is general over Europe, both at Nordic sites (shown in the second row in Figure 4.5), central European sites (in the third row) and on Southern European sites (in fourth row).

Since the emissions used by OsloCTM2 in Europe based on the RETRO data set are higher than the EMEP emissions, used by the global EMEP model, this could to a certain extent justify why the calculated air concentrations from the OsloCTM2 model are higher than the EMEP model values. However, the comparison of the two models performance in other areas reinforces the impression that this is more a general feature of the OsloCTM2 model, probably related to vertical exchange and its parametrization of dry and wet deposition. For example, Table 4.2 shows the comparison of model results from OsloCTM2 and EMEP global with observations over East Asia. Over East Asia, the sulphur dioxide emissions used by the OsloCTM2 are generally significantly

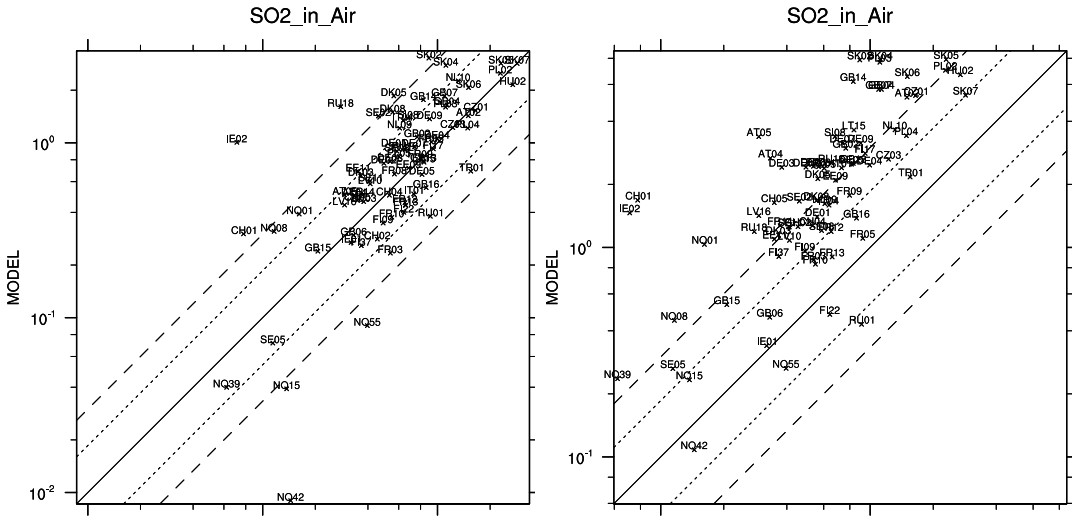

(a) **EMEP** (Obs. 0.75, Mod. 0.96, corr 0.73) (b) **CTM2** (Obs. 0.75, Mod. 2.50, corr 0.73)

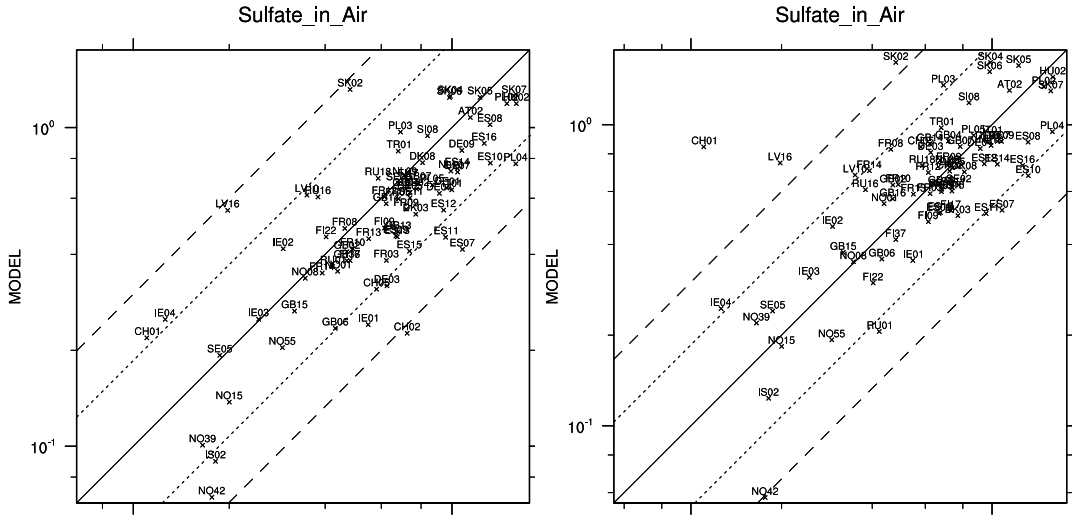

(c) **EMEP** (Obs. 0.70, Mod. 0.58, corr 0.75) (d) **CTM2** (Obs. 0.70, Mod. 0.71, corr 0.64)

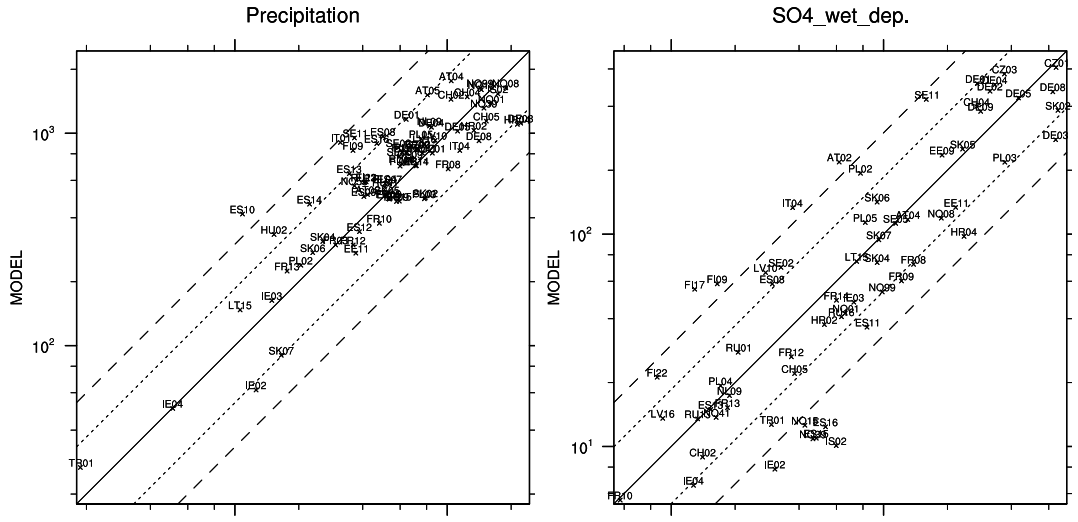

(e) **EMEP** (Obs. 53268, Mod. 56817, corr 0.79) (f) **EMEP** (Obs. 8773, Mod. 8819, corr 0.82)

Figure 4.4: Annual scatter plots for different sulphur compounds measured at European EMEP stations. Units: μg(S)m^{-3} for air concentrations, mm for precipitation and mg(S)m^{-2} for depositions.

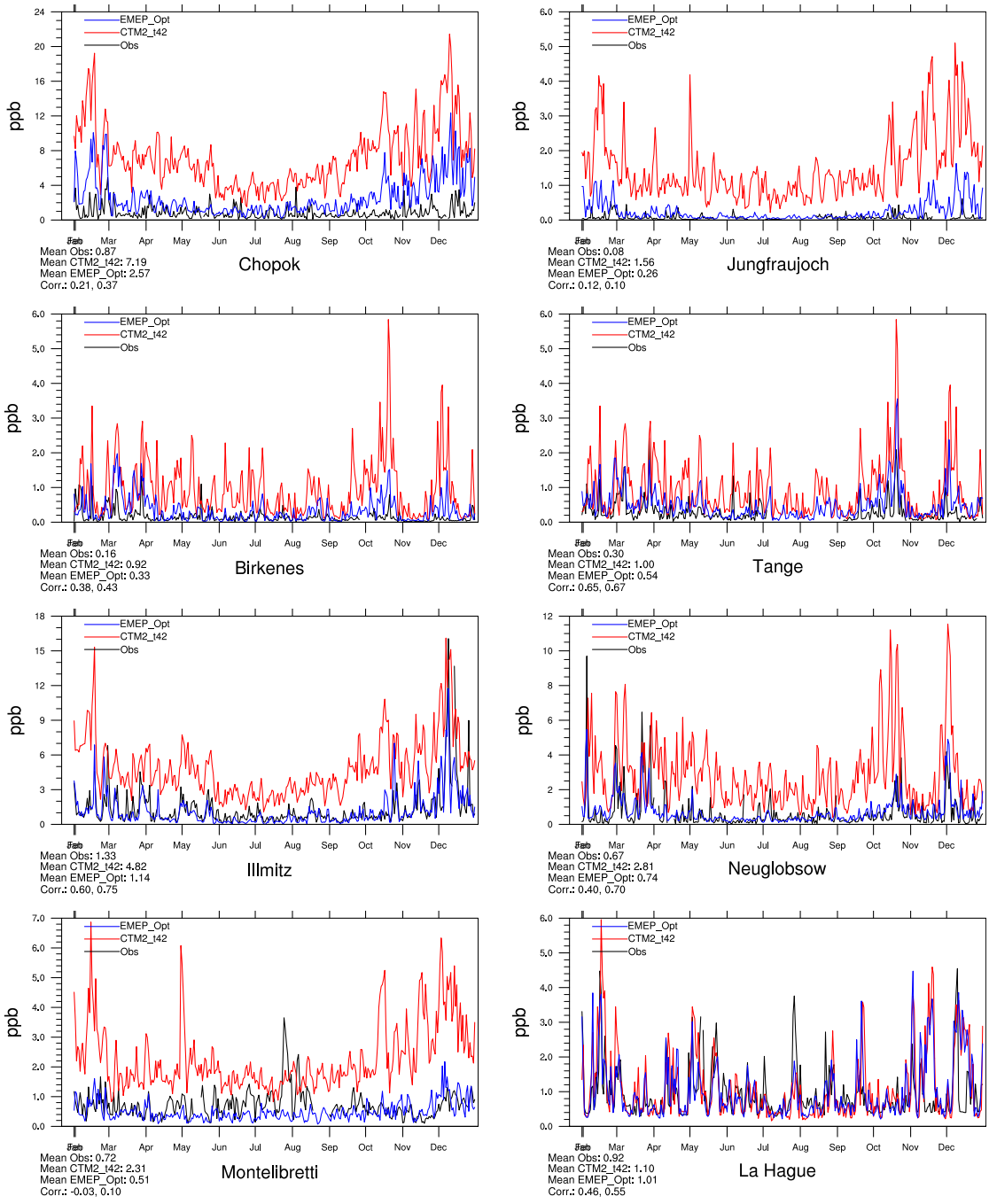

Figure 4.5: Annual timeseries of daily SO_2 surface mixing ratio (ppbv) over selected European stations.

lower than the ACESS emissions used by EMEP and still the concentrations calculated by the OsloCTM2 model are higher than those calculated by EMEP. This indicates that the tendency to overestimate sulphur dioxide emissions in the OsloCTM2 model is likely to be a systematic feature of the model and not only due to the emission input.

It is also worth mentioning that the performance of both global models in Asia is much worse than over Europe. Measurements of SO_2 in East Asia on a daily basis are available from EANET (Acid Deposition Monitoring Network in East Asia). We have limited experience with the representativeness and quality of this data set. The same applies also to the quality of the emission data, its sectoral, temporal and spatial distribution. Consequently, for a further interpretation of these results more insight is needed with regard to measurement location, measurement methods and distance to major source areas over Asia.

4.1.4 Nitrogen species

The performance of the global models for nitrogen compounds has been evaluated over Europe and Asia using measurement data from the EMEP and EANET networks. Over Europe, the comparison extends to nitrogen dioxide, wet depositions of oxidized and reduced nitrogen, concentrations of ammonia and ammonium in air and total nitrate (particulate nitrate and HNO_3) concentrations in air. Figure 4.6 shows annual scatter plots of nitrogen dioxide for both the global EMEP and the OsloCTM2 models while the other nitrogen components are only analyzed for the EMEP model since such output data is not available for OsloCTM2. Time series of modeled and observed concentrations of NO_2 over selected European stations are presented in Figure 4.7. Over Asia, daily measurements of NO_2 compiled by the EANET network are presented in Table 4.3.

Over Asia, measured concentrations of NO_2 are generally much higher than calculated by both models and considerably higher than concentrations meausured over Europe, suggesting a substantial influence from local sources. For further interpretation of these measurements more insight is needed with regard to the quality of the measurements, the measurement location and distance to major source areas, as already discussed in Chapter 3.

Over Europe, the global EMEP model tends to underestimate NO_2 concentrations while the OsloCTM2 model tends to overestimate surface NO_2 concentrations, despite using lower emissions than the EMEP model. As indicated in Chapter 3, this systematic behavior in the OsloCTM2 model is likely to be related with the parametrization of vertical exchange and the treatment of dry and wet deposition in the model.

The performance of the global EMEP model is very similar to that of the hemispheric model (Jonson et al. 2006), and very close also to the performance of the EMEP regional model. The only possible difference is an improvement in the description of wet deposition values, mostly associated to the improved precipitation fields when using ECMWF meteorology as opposed to the PARLAM data used to drive the regional EMEP model. The use of coarser resolution in the global model as compared

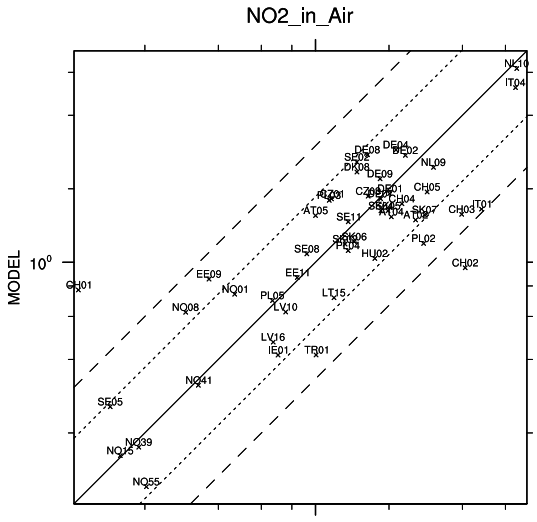

(a) **EMEP** (Obs. 1.75, Mod. 1.51, corr 0.79)

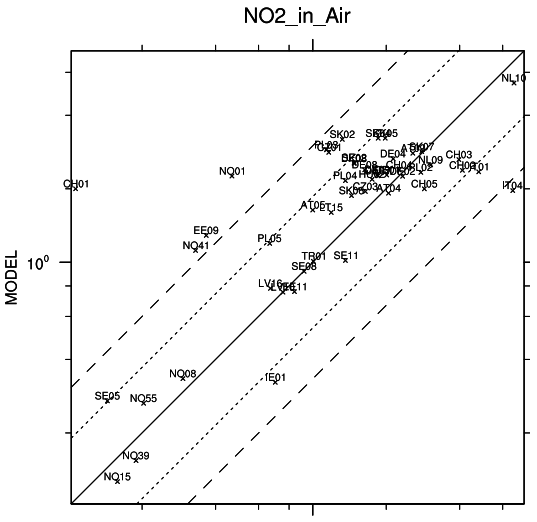

(b) **CTM2** (Obs. 1.75, Mod. 1.92, corr 0.65)

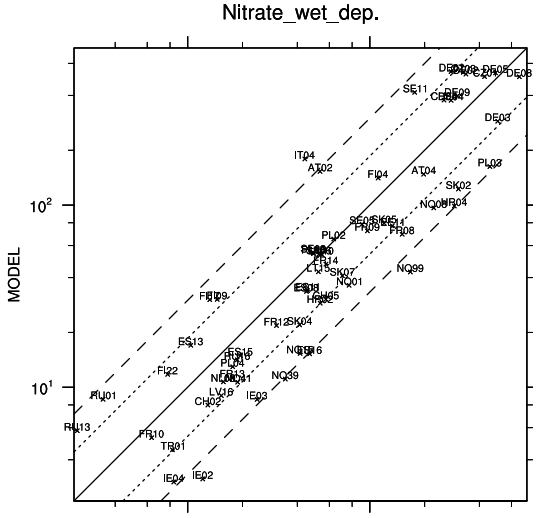

(c) **EMEP** (Obs. 7652, Mod. 7404, corr 0.82)

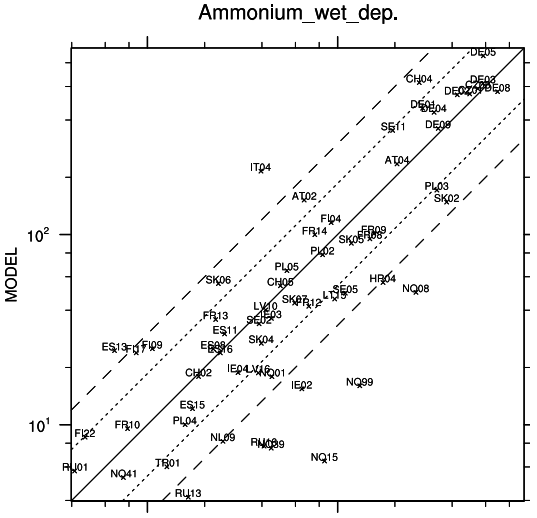

(d) **EMEP**(Obs. 8773, Mod. 8819, corr 0.73)

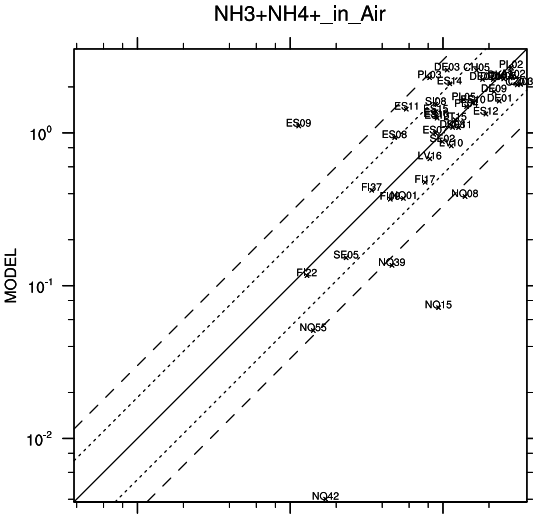

(e) **EMEP** (Obs. 1.26, Mod. 1.29, corr 0.74)

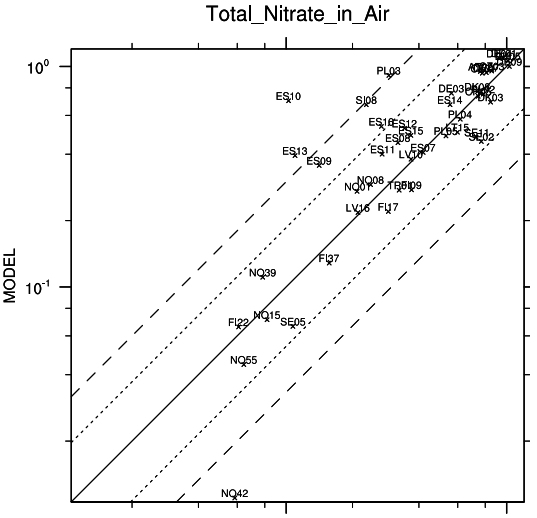

(f) **CTM2** (Obs. 0.46, Mod. 0.53, corr 0.83)

Figure 4.6: Annual scatter plots for different nitrogen compounds measured at European EMEP stations. Units: μg(N)m^{-3} for air concentrations and mg(N)m^{-2} for depositions.

to the regional EMEP model does not seem to play a significant role for the performance of the EMEP model.

In order to check whether this is also the case for the OsloCTM2 model, selected periods in January and July have been run with 1° x 1° resolution. Starting from initial fields created by a multi-year T42 run, two short-term runs have been performed with the OsloCTM2 model. The first one from Jan 7, 2001 - Jan 21, 2001 and the second one from July 7, 2001 - July 21, 2001. From both runs, the last ten days have been used for analysis. The evaluation of model performance presented here focuses on NO_2 surface measurements only, but a large data set has been generated including hourly 3-D fields of ozone and NO_2, which will be further investigated in the near future. In some cases 1° x 1° is higher than T42, in other cases lower, depending on whether or not the 1° x 1° part of the T42 box is above or below average. For instance, in cases where a point source of emissions is located within a 1° x 1° box it will represent a peak, which is smoothed out in the corresponding T42 box. In cases where the emission in the 1° x 1° box is low, it would tend to yield lower values than in the T42 box. However it can be noted that the pattern of variation is largely the same. In some cases, where it is not the same, small scale meteorological conditions, which are not necessarily synchronous with the T42 conditions, could explain the differences.

Table 4.3: Comparison of Modeled Versus Observed NO_2 for Year 2001 for EANET stations. Concentrations are 12-monthly Means of daily values.

Station	Obs.	EMEP_global		OsloCTM2	
NO_2	μg(N)m^{-3}	μg(N)m^{-3}	r	μg(N)m^{-3}	r
Hongwen	11.36	0.94	0.10	1.06	0.20
Xian (Xiangzhou)	19.10	2.23	0.14	0.43	0.18
Jinyunshan	2.40	1.71	0.10	4.56	0.22
Weishuiyuan	4.64	2.25	-0.08	2.73	-0.03
Banryu (Japan)	3.94	0.76	-0.15	0.44	0.17

Comparison of these model results with observations are shown in figures 4.8 and 4.9. From these it is not easy to say whether the resolution of the model is a reason for the overestimation in case of CTM2_t42, because a finer resolution does not give much better fit with observations. In many of the stations CTM2_1X1 mean values are much higher than those of CTM2_t42 in both episodes of January and July. Further evaluation and longer term runs will be needed to draw firm conclusions from the OsloCTM2 results with finer resolution.

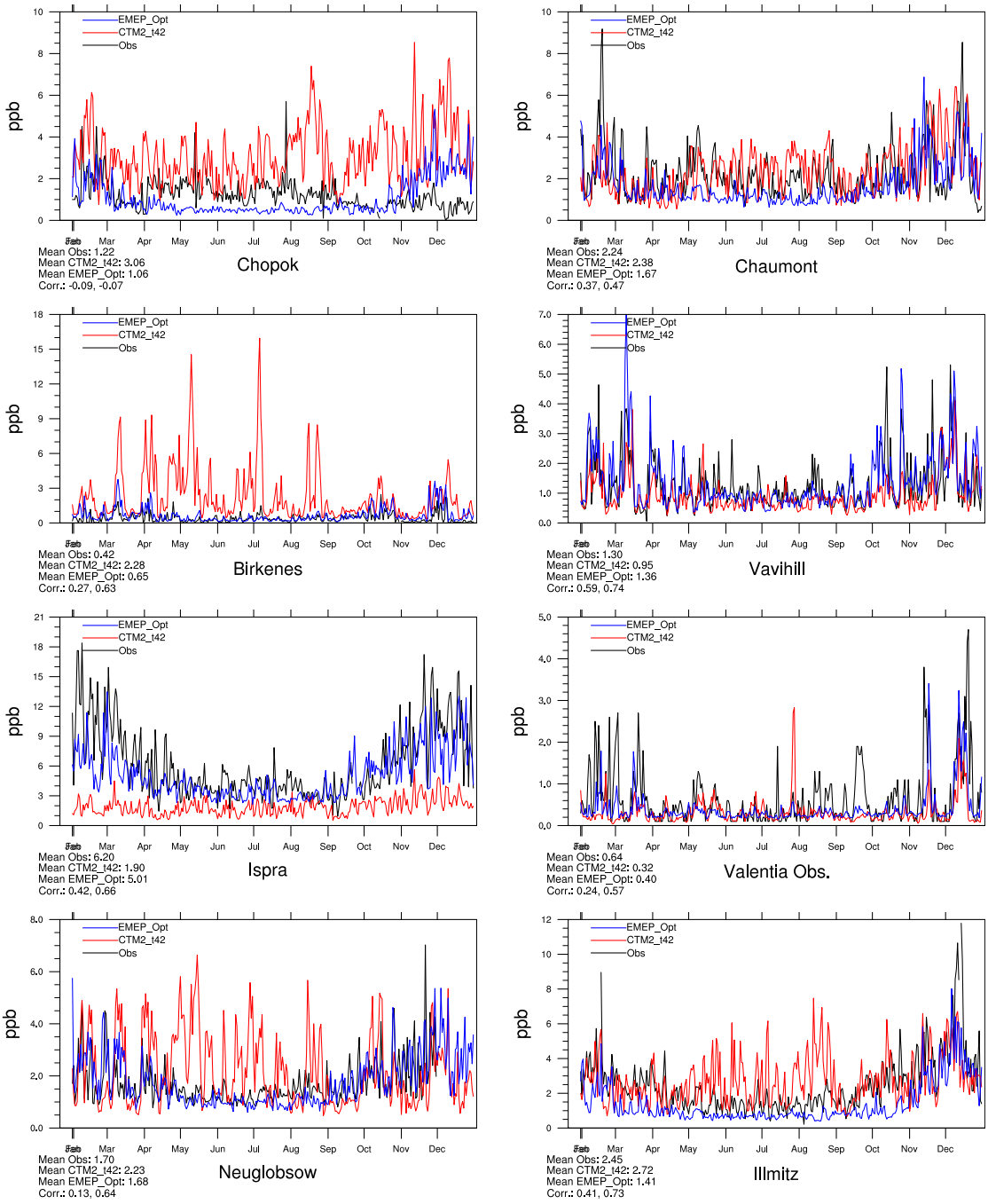

Figure 4.7: Time series of Modeled versus Observed Daily mean NO_2 (ppb) in selected European stations.

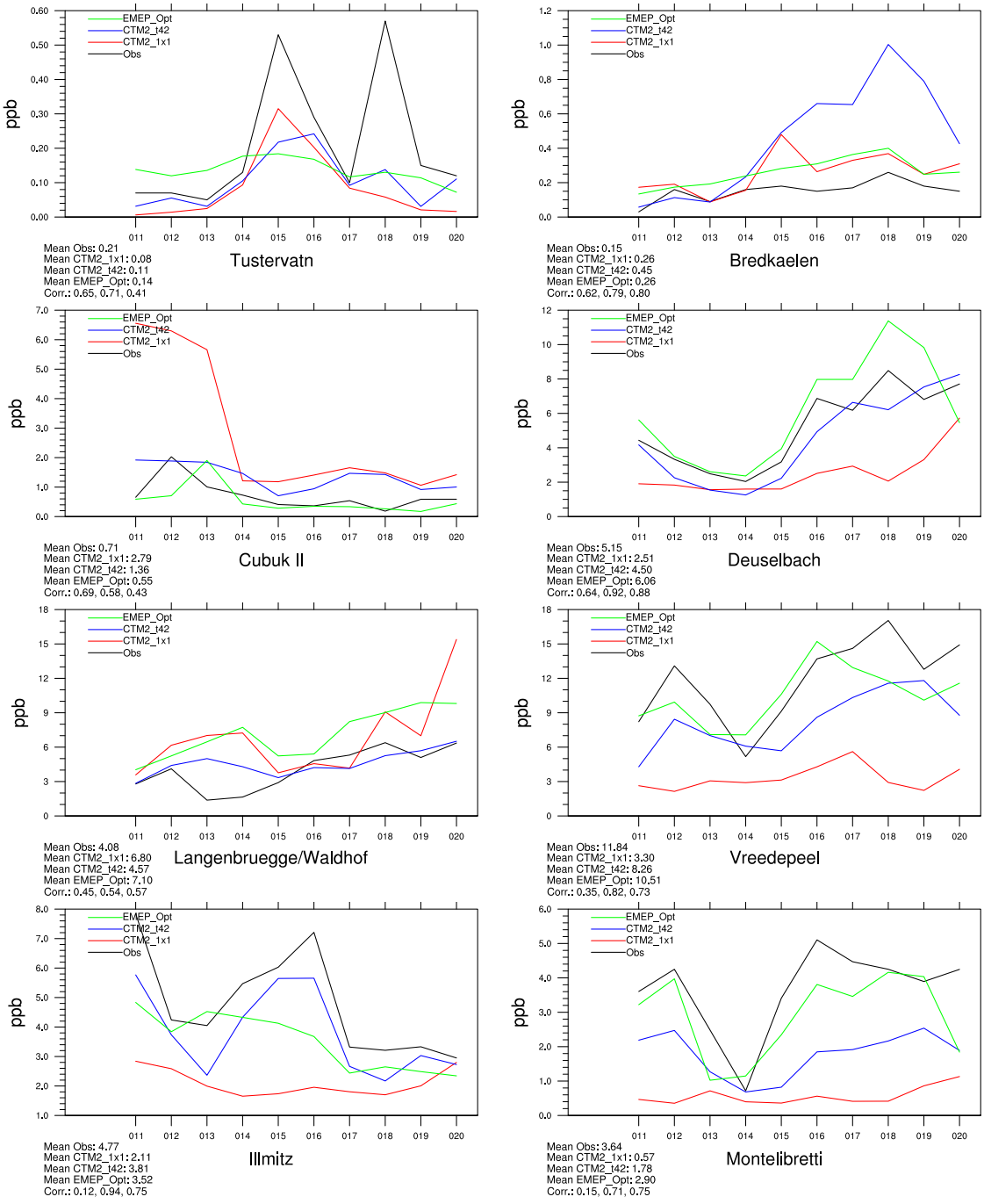

Figure 4.8: Modeled versus Observed Daily mean NO_2 (ppb) for 2-week period in January 2001. Observations are in black, EMEP global model results in green, OsloCTM2 results with T42 resolution in blue and OsloCTM2 results with 1° x 1° resolution in red.

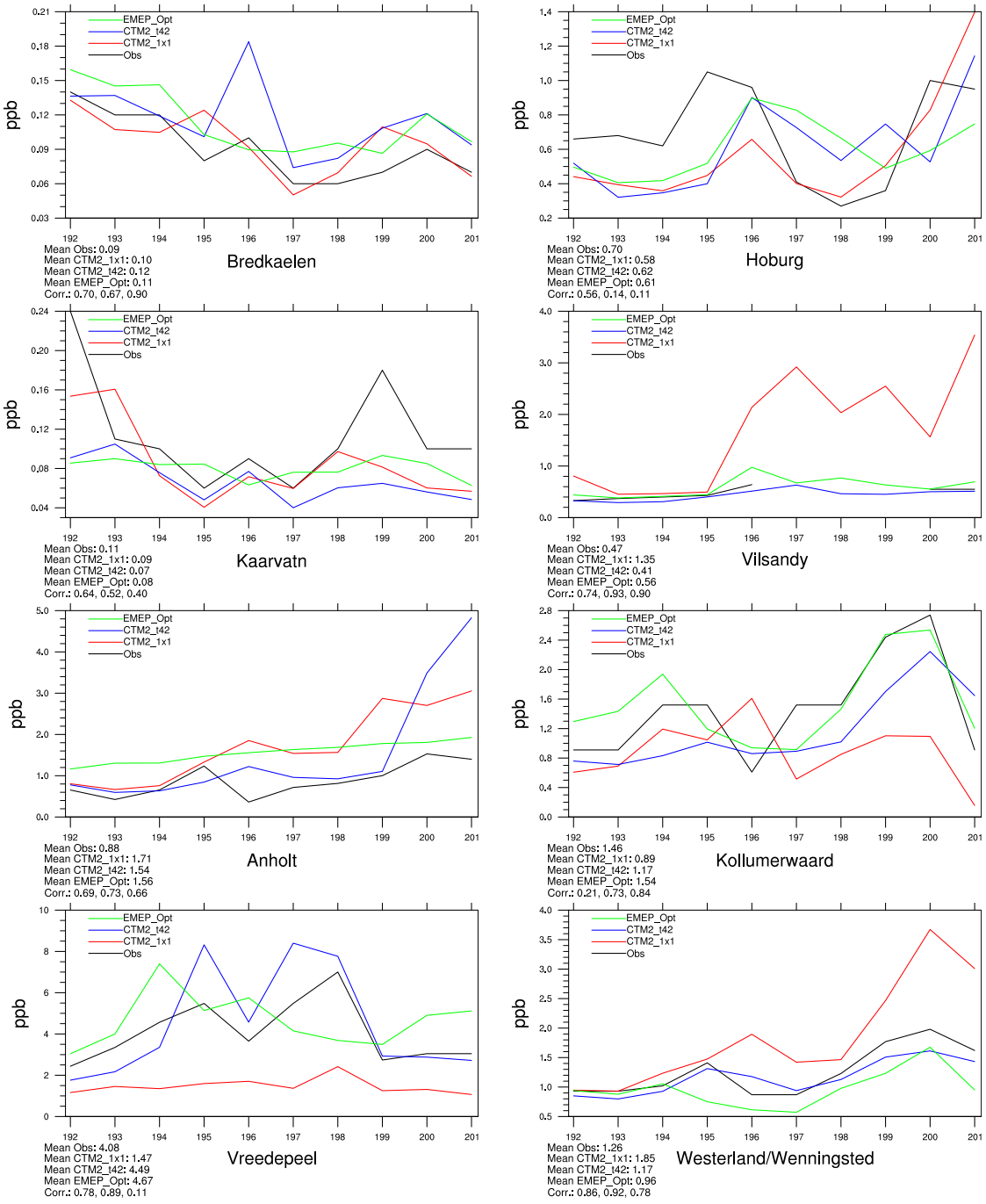

Figure 4.9: Modeled versus Observed Daily mean NO_2 (ppb) for 2-week period in July 2001. Observations are in black, EMEP global model results in green, OsloCTM2 results with T42 resolution in blue and OsloCTM2 results with 1° x 1° in red.

4.2 Vertical profiles

4.2.1 Ozone sondes

In this section output from the two models are compared to ozone soundings. As it turns out, there are only small differences between the global calculations presented in this report and results from the hemispheric model version presented last year in Jonson et al. (2006). For the OsloCTM2 model results are virtually unchanged. Therefore only a limited selection of sondes are presented in Figure 4.10. The graphs show the average for all sonde measurements available for the selected sites in the chosen month. The horizontal bars shows the range of measured and calculated ozone levels between the individual sondes included in the average.

Again both models reproduce the measured ozone levels in the free troposphere nicely in the winter months. At this time of the year the variability between the individual sondes is small. As for the hemispheric model version the global EMEP model underestimates ozone in the free troposphere in the summer months. This underestimation is not seen in the OsloCTM2 model results. A likely cause of this underestimation is that convective transport is not adequately described in the EMEP model. Also, ozone imported from the stratosphere could be too low. Plans for including a parametrization of convective transport similar to what is used in OsloCTM2 are described in Chapter 5. In polar regions ozone is underestimated by both models in the free and upper troposphere, and by the OsloCTM2 model, also in the boundary layer. Especially in high altitudes this could be due to too little ozone destruction in the Arctic stratosphere. It is recommended to investigate the reasons for this behavior further in terms of boundary layer height/mixing, dry deposition parametrization and transport from lower latitudes.

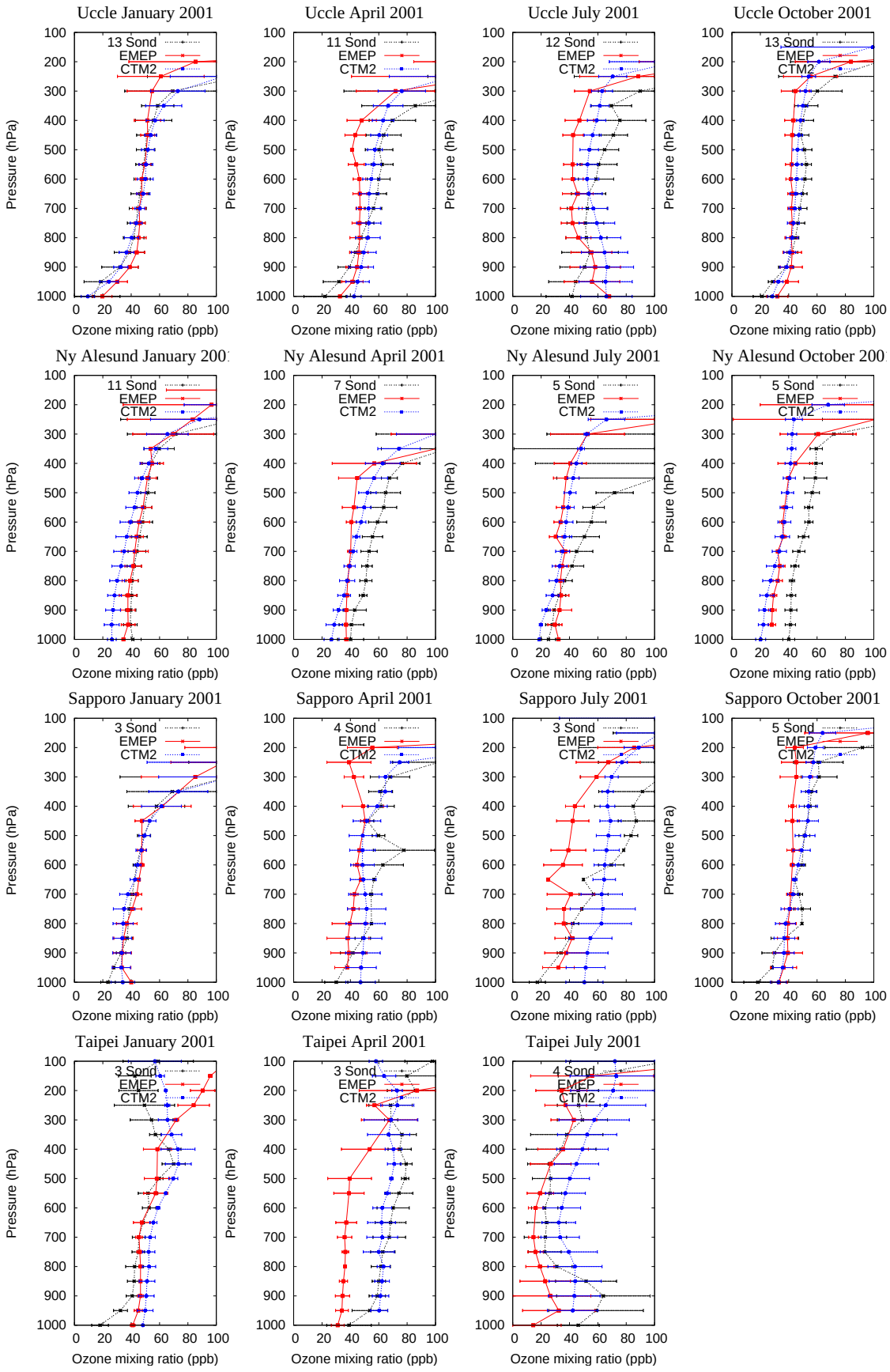

Figure 4.10: Model calculated ozone, and ozone sonde measurements for European sites, averaged for all available sonde measurements in the individual months shown.

CHAPTER 5

On-going model development: convection in the OsloCTM2 and EMEP models

5.1 Convection in the atmosphere

Convection is an effective process for vertical exchange of heat, momentum and mass. In the atmosphere it is most often caused by solar heating of the surface, especially in low latitudes. The chain of processes can be briefly summarized as follows: near-surface air is heated by sunlight → the air density decreases → convective instability → upward motion of air and vertical mixing of tracers. The vertical flow is generally further enhanced by the release of heat when humidity in the rising air condenses.

The importance for atmospheric chemistry, air pollution and climate derives primarily from the fact that convective processes can transport near-surface pollutants more rapidly into the free troposphere than large scale motion. A well-known example are ozone precursors such as NOx and hydrocarbons, which have major emission sources at the surface and exhibit a non-linear behavior in terms of ozone-production efficiency. Transported into the free troposphere, NOx has a larger ozone yield per molecule than at the surface where concentrations are higher. The upper troposphere is limited in hydrocarbons, so that transport from the surface has the overall effect of increasing ozone atop convective cells.

In addition, vertical transport of air often leads to convective rainfall by which water-soluble gases and particles are washed out (wet deposition) and efficiently transported through the atmospheric column, and in many cases removed completely by rain reaching the surface.

However, vertical transport is important not only for the height distribution of concentrations and chemical production/destruction efficiencies, but also for long-range transport. Large-scale flow occurs primarily in the free troposphere. Convective events

efficiently move pollutants from the boundary layer into the free troposphere where they can be readily transported over large distances, dependent on their chemical lifetimes and water solubilities.

In air pollution and climate models, convection is usually grid-resolved in the vertical, but sub-grid in the horizontal dimensions. This fact, combined with the importance of convection for distribution of gases and particles, calls for parametrization that relate convective transport and washout to other fields that are grid-resolved.

5.2 Implementation in the OsloCTM2 model

In a chemical transport model we need to distinguish three steps: a) the process of convection as predicted by a meteorological model, b) the vertical transport of humidity, gases and particles in grid columns with convective activity, based on fields of motion from the underlying meteorological model, and c) the uptake of water-soluble gases or particles, often followed by rain-out. In the case of OsloCTM2 these three steps are realized by:

1) The convective mass flux scheme at ECMWF
- applied in the Integrated Forecast System (IFS) Model when generating wind fields for OsloCTM2
- developed by Tiedtke (Tiedtke, 1989), and further refined later
- output: convective mass fluxes, convective rain

2) Convective transport of chemical species (applied in OsloCTM2)
- developed by M. Prather and B. Hannegan, University of California at Irvine (UCI)
- using the vertical gradient of convective mass fluxes together with mixing ratios information and second-order moments

3) Convective washout (OsloCTM2)
- implemented by T. Berntsen (University of Oslo), described by (Berglen et al. 2004)
- using temperature, pressure, specific humidity, large scale rain, convective rain, and convective mass flux provided by ECMWF

The mathematical background of the mass flux scheme used in the IFS model is briefly summarized in the following. The vertical convective transport of a quantity φ can be written as the sum of an updraft term and the lateral detrainment/entrainment terms:

$$-\frac{1}{\rho}\frac{\partial(\rho\overline{w'\varphi'})}{\partial z} = -\frac{1}{\rho}\left(\frac{\partial(M_u\varphi_u)}{\partial z} + \frac{\partial(M_d\varphi_d)}{\partial z} + \frac{\partial(M_e\varphi_e)}{\partial z}\right)$$

ρ: density, φ: quantity transported (e.g. tracer mixing ratio), M: air mass, z: vertical coordinate. Index u: updraft, index d: detrainment, index e: entrainment.

The main goal from a modeling point of view is to derive detrainment and en-

trainment from the mean flow based on empirical data, so that the vertical convective mass flux can be calculated. The Tiedtke scheme considers a population of convective clouds where the cloud ensemble is described by a one-dimensional bulk model. Different kinds of convection are considered:

deep convection :
- extending from the boundary layer to the upper troposphere
- connected with large-scale convergent flow
- maintained by large-scale moisture convergence
- accompanied by precipitation

mid-level convection :
- extending from one atmospheric layer (above the boundary layer) to another
- connected with potentially unstable air above the boundary layer
- maintained by large-scale moisture convergence

shallow convection :
- trade-wind cumuli are one example of this type of convection
- mostly non-precipitating, maintained by supply of moisture from surface evaporation.

In the mass flux scheme the vertical gradient of vertical upward mass flux equals the entrainment minus the detrainment in the box:

$\frac{\partial M_u}{\partial z}$=$E_u$-$D_u$

Starting from this formula E_u can be further subdivided into

E_u=E_u^1+E_u^2 where E_u^1 : turbulent flow, and E_u^2 : organized flow

These two terms can be written as E_u^1=$\epsilon_u M_u$, E_u^2=-$\frac{\bar{\rho}}{\bar{q}}$ ($\bar{v}\cdot\nabla\bar{q}$ +$\bar{w}\frac{\partial\bar{q}}{\partial z}$), and ϵ_u=$\frac{0.2}{R_u}$

The estimation of ϵ_u is where the cloud model comes into play. The following approximations can be made under different conditions:
ϵ_u= 1 x $10^{-4}m^{-1}$ for deep and mid level convection in the presence of large-scale flow convergence and
ϵ_u= 3 x $10^{-4}m^{-1}$ for shallow convection in suppressed conditions.

Similar equations can be derived for updraft detrainment, and downdraft both entrainment and detrainment.

Once the vertical mass flux is in place, convective transport of species can be calculated in the CTM. In OsloCTM2 this is currently done with a time step of 1 hour. The

so-called elevator principle is used (elevator = updraft core). The elevator stops at each model level. Air, humidity, chemical species, and particles get on or off, depending on the vertical gradient of convective mass flux. This is illustrated in Figure 5.1.

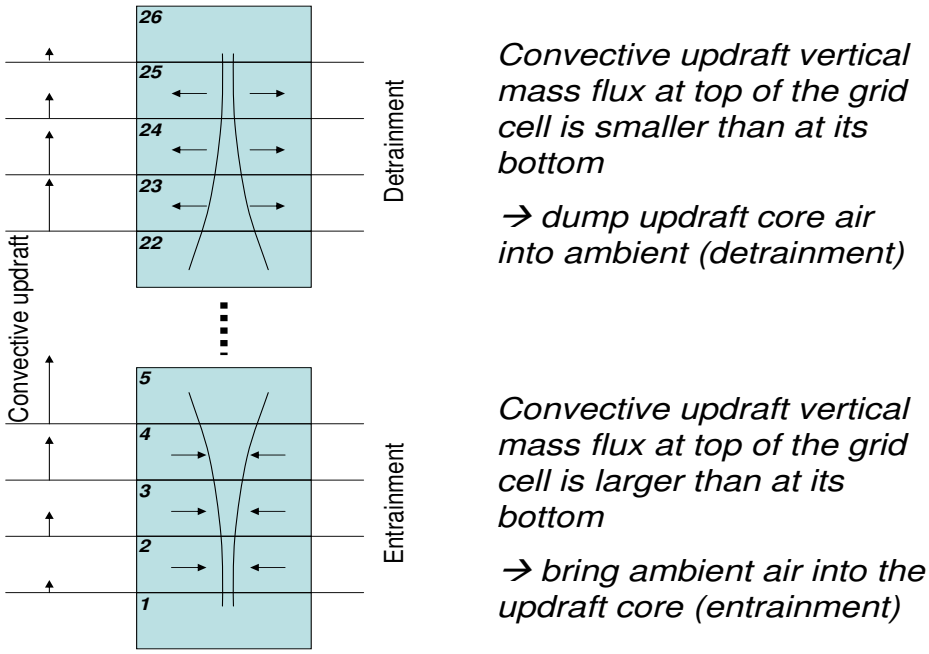

Figure 5.1: Illustration of updrafts. Convective downdrafts are treated similarly

If the vertical updraft decreases with altitude, as illustrated by the left arrows in the upper part of the figure, then more air is entering the convection core from below the grid box than exiting at the top. This must be compensated by horizontal detrainment from the convective cell into the ambient air (i.e. the elevator). In the case of updraft flux increasing with height, as illustrated by the bottom part of the figure, there will be a deficit in the core, compensated by entrainment from ambient air (i.e. the elevator). The entrainments and detrainments can thus be quantified for each grid box characterized by non-zero convective mass flux based on the vertical gradient of the mass flux. Starting from these quantities, convective washout of species is calculated with a time step of 3 hours, involving the following steps:

a) calculate the air mass in the elevator (from temperature and geometry of the grid box)
b) calculate water mass in the elevator (from humidity)
c) calculate temperature of elevator (mass weighted mean of what comes from below and what is entrained) → some water will condensate/evaporate

d) find fraction of water vapor and cloud droplets (iterative process)
e) convective rain-out is known from ECMWF IFS → can calculate how large a fraction of the available cloud droplets are lost
f) translate water loss into species loss using Henry's law constants

5.3 Implementation in the EMEP model

As of today, convective transport is treated in the EMEP model as part of the vertical exchange routine, with effective vertical diffusion coefficients. Previously this method has been sufficient as EMEP focused on regions where vigorous convective events are rare. However, in a global model comprising equatorial regions and assessing long-range transport of pollutants also in low latitude regions, a more adequate parametrization of convection is necessary.

All meteorological parameters needed, such as upward vertical mass flux, rain, etc. have already been downloaded from ECMWF and are ready to be used in the global EMEP model version that is driven by ECMWF data. However, the implementation of the Prather code, which is used in OsloCTM2, is not straight-forward as EMEP uses a different advection transport scheme.

Furthermore, other EMEP applications feature higher resolutions down to a few kilometers, where convection may be partly grid-resolved. This requires flexible coding, so that the same convection routine in the global EMEP model version can also be used in regional and local scale applications. At high resolution the vertical updraft can be calculated from horizontal wind convergence. To create a flexible code, convection and advection can be combined and done at the same time in one routine even in a course-resolution model. This method is currently being tested in a CTM at UCIrvine and could, if successful, represent a promising approach for the implementation of convection in the EMEP model.

As explained above, work to improve the convection parametrization in EMEP is just initiated and progress will be reported in due time.

.

CHAPTER 6

Conclusions and recommendations

For the first time results from one year of calculations with the global EMEP model have been presented here and compared with results from the global OsloCTM2 model developed at the University of Oslo. The performance of these models has also been evaluated against measurements from different sources, including ground level data, ozone sonde data and satellite observations.

The global EMEP model uses a horizontal resolution of 1° x 1° while for this study the OsloCTM2 model has been run with T42 resolution (about 2.8° x 2.8°). In order to investigate to what extent differences in model resolution affect the performance of the models, it was initially envisaged to run the OsloCTM2 model for an entire year with the same resolution as the global EMEP model. Due to the high CPU requirements of the OsloCTM2, however, the runs with 1° x 1° resolution were limited to two separate 2-week periods in January 2001 and July 2001, respectively (the OsloCTM2 model uses about 30 times more CPU resources than the EMEP global model, mainly due to the use of the highly accurate second order moment scheme for advection and the inclusion of comprehensive stratospheric chemistry). First comparisons with these runs are shown in this report and further evaluation and longer term runs will be needed to draw firm conclusions from the OsloCTM2 results with finer resolution.

For surface ozone, the two global models show very similar performance and are able to reproduce the observed spatial gradients and seasonal variations over the analyzed sites. The OsloCTM2 model appears to perform better in mountain regions such as the Alps, whereas the EMEP global model appears to perform better in western Europe, most likely associated to that the model uses better emission data in the European region. The evaluation of sulphur components shows a systematic overestimation of sulphur dioxide concentrations for OsloCTM2. The overestimation is by a factor of 3 over Europe and even higher over Asia. This contrasts with the performance of the global EMEP model which is generally in better agreement with measurements

of sulphur dioxide and sulphate both in air and precipitation. In Europe, the emissions used by OsloCTM2 based on the RETRO data set are higher than the EMEP emissions, used by the global EMEP model. This could to a certain extent justify why the calculated air concentrations from the OsloCTM2 model are higher than the EMEP model values. However, over Asia the sulphur dioxide emissions used by OsloCTM2 are generally significantly lower than the ACESS emissions used by EMEP and still the concentrations calculated by the OsloCTM2 model are higher than those calculated by EMEP. This indicates that the tendency to overestimate sulphur dioxide emissions in the OsloCTM2 model is likely to be a systematic feature of the model and not only due to the emission input. The same tendency of the OsloCTM2 model to overestimate surface concentrations of primary gases is observed also for nitrogen dioxide. Both nitrogen dioxide surface concentrations and total column values for NO_2 are higher in the OsloCTM2 model than in the global EMEP model and overestimate the observations. The reasons for this behavior are not clear but they are likely associated with the OsloCTM2 parametrization of vertical exchange and the treatment of dry deposition.

For both models, the performance over Europe is generally better than for other regions. This is likely because the input data and to a certain extent also the measurement data available for this report have higher quality over Europe than in other studied areas. Surprisingly, however, this is not the case for CO, where the two models perform better over Asian stations than over European sites. This needs to be further analyzed with an extended set of observations.

It is reassuring that the performance of the global EMEP model is very similar over Europe to the performance of the regional EMEP model. This was to be expected since differences in model performance between the regional and the global model are only due to differences in the resolution and accuracy of the meteorological input data. The fact that the two models have such similar performance over Europe is an indication that the flexible modelling system is functioning as expected. A different issue is the need for introducing improvements in the parametrizations of certain processes in the EMEP model to allow a better characterization of global scale pollution transport.

The present evaluation has identified problems with both models that need to be further investigated. The global EMEP model performs worse in areas affected by deep convection and tends to underestimate free tropospheric levels of ozone. Such behavior was already identified last year with the evaluation of the hemispheric version of the model. The same conclusions are valid for the global model version and current model development for the EMEP model is already addressing the improvement of the parametrization of convective processes in the model and the description of stratospheric exchange.

The OsloCTM2 model has problems with large underestimations in polar regions for ozone and it shows a general overestimation of surface concentration of primary gases. There are indications that this behavior of the model is associated with the parametrization of vertical exchange and dry deposition in the model. Work is planned for the near future to compare dry deposition schemes between the OsloCTM2 model and the EMEP model to allow the further implementation of the EMEP scheme in the

OsloCTM2 model.

The evaluation has also identified a series of questions on the input emission and measurement data over Asia. The poor model performance for sulphur and nitrogen components over Asia for the two models as well as large underestimations by the two global models of the observed NO_2 concentrations over Asia recommended further analysis. It is envisaged that further co-operation within the TFHTAP will help elucidate the reasons for such poor model behavior in this area.

References

C.M. Benkovitz, M.T. Scholtz, J. Pacyna, L. Tarrasón, J. Dignon, E.C. Voldner, P.A. Spiro, J.A. Logan, and T.E. Graedel. Global gridded inventories for anthropogenic emissions of sulfur and nitrogen. *J. Geophys. Res.*, 101:29,239–29,253, 1996.

T. F. Berglen, T. K. Berntsen, I. S. A. Isaksen, and J. K. Sundet. A global model of the coupled sulfur/oxidant chemistry in the troposphere: The sulfur cycle. *J. Geophys. Res.*, 109, 2004. doi:10.1029/2003JD003948.

T. K. Berntsen and I. S. A. Isaksen. A global 3D chemical transport model for the troposphere: Model description and CO and O_3 results. *J. Geophys. Res.*, 102: 21,239–21,280, 1997.

T.K. Berntsen and I.S.A. Isaksen. Effects of lightning and convection on changes in upper tropospheric ozone due to aircraft. *Tellus*, 51B:766–788, 1999.

A. Bott. A positive definite advection scheme obtained by non-linear re-normalization of the advection fluxes. *Monthly Weather Review*, 117:1,006–1,015, 1989.

D. Fowler and J.W. Erisman. Biosphere/Atmosphere Exchange of Pollutants. In P.M. Midgley and M. Reuter, editors, *Towards Cleaner Air for Europe – Science, Tools and Applications, Part 2. Overview of subproject BIATEX-2. Overviews from the Final Reports of the EUROTRAC-2 Subprojects*. Margraf Verlag, Weikersheim, 2003, 2003. Also available from http://www.gsf.de/eurotrac/publications/.

A.A.M. Holtslag, E.I.F. DrBruijn, and H.-l. Plan. A high resolution air mass transformation model for short-range weather forecasting. *Monthly Weather Review*, 118: 1561–1575, 1990.

I.S.A. Isaksen, B. Rognerud, F. Stordal, M.T. Coffey, and W.G. Mankin. Studies of arctic stratospheric ozone ozone in a 2-d model including some effects of zonal asymmetries. *Geophys. Res. Lett.*, 17:557–560, 1990.

J. E. Jonson, P Wind, M. Gauss, S. Tsyro, O.A. Søvde, H. Klein, I.S.A. Isaksen, and L. Tarrasón. First results from the hemispheric EMEP model and comparison with the global Oslo CTM2 model. EMEP/MSC-W note 2/06, The Norwegian Meteorological Institute, Oslo, Norway, 2006.

S.M Metzger, F.J. Dentener, J. Lelieveld, and S.N. Pandis. Gas/Aerosol Partitioning 1. A computationally efficient model. *J. Geophys. Res.*, 107(D16):ACH16, 2002a.

S.M Metzger, F.J. Dentener, A. Jeuken, M. Krol, and J. Lelieveld. Gas/Aerosol Partitioning 2. Global modelling results. *J. Geophys. Res.*, 107(D16):ACH17, 2002b.

E. Nemitz, C. Milford, and M.A. Sutton. A two-level canopy compensation point model for describing bi-directional biosphere-atmosphere exchange of ammonia. *Q. J. R. Meteorol. Soc.*, 127:815–833, 2001.

J. Olivier, J. Peters, C. Granier, G. Ptron, J. F. Mller, and S. Wallens. Present and future surface emissions of atmospheric compounds. In *POET Rep. 2*. EU Proj. EVK-1999-00011, Eur. Union, Brussels, 2003.

J.G.J. Olivier and J.J.M. Berdowski. Global emissions sources and sinks. In J.J.M. Berdowski, R. Guicherit, and B.J Heij, editors, *The Climate System*, pages 33–78. A.A Balkema Publishers/Sweets & Zeitlinger Puplishers, Lisse, The Netherlands, 2001.

M.J. Prather. Numerical advection by conservation of second order moments. *J. Geophys. Res.*, 91:6,671–6,681, 1986.

C. Price, M.J. Prather, and J. Penner. NO_x from lightning, 1, Global distribution based on lightning. *J. Geophys. Res.*, 102:5,929–5,942, 1997a.

C. Price, M.J. Prather, and J. Penner. NO_x from lightning, 2, Global distribution based on lightning. *J. Geophys. Res.*, 102:5,943–5,952, 1997b.

D. Simpson, A. Guenther, C. N. Hewitt, and R. Steinberger. Biogenic emissions in Europe 1. Estimates and uncertainties. *J. Geophys. Res.*, 100:22,875–22,890, 1995.

D. Simpson, H. Fagerli, J.E. Jonson, S. Tsyro, P. Wind, and J-P. Tuovinen. Transboundary acidification, eutrophication and ground level ozone in Europe, PART 1. Emep status report 1/2003, The Norwegian Meteorological Institute, Oslo, Norway, 2003.

L.H. Slørdal, H. Laupsa, P. Wind, and L. Tarrasón. Local and regional description of particulate matter in the oslo area. Joint MSC-W and NILU technical report, MSC-W technical report 5/2004, The Norwegian Meteorological Institute, Oslo, Norway, 2004.

Frode Stordal, Ivar S. A Isaksen, and Kjell Horntveth. A diabatic circulation two–dimensional model with photochemistry: simulations of ozone and long–lived tracers with surface sources. *J. Geophys. Res.*, 90:5,757–5,776, 1985.

D.G. Streets, T.C. Bond, G. R. Carmichael, S. D. Fernandes, Q. Fu, D. He, Z. Klimont, S. M. Nelson, N. Y. Tsai, M. Q. Wang, J.-H. Woo, and K. F. Yarber. An inventory of gaseous and primary aerosol emissions in Asia in the year 2000. *J. Geophys. Res.*, 108, 2003. doi:10.1029/2002JD003093.

M. Tiedtke. A comprehensive mass flux scheme for cumulus parameterisation on large scale models. *Monthly Weather Review*, 117:1,779–1,800, 1989.

V. Vestreng, K. Mareckova, S. Kakareka, A. Malchykhina, and T. Kukharchyk. Inventory review 2007: Emission data reported to CLRTAP convention and NEC directive. Stage 1 and 2 review. Review of gridded data and Review of PM inventories in Belarus, Republic of Moldova, Russian Federation and Ukraine. EMEP/MSC-W technical report 1/2007, The Norwegian Meteorological Institute, Oslo, Norway, 2007.

Y. Wang, M.B. McElroy, R.V. Martin, D.G. Streets, Q. Zhang, and T.-M Fu. Seasonal variability of NOx emissions over east China constrained by satellite observations: Implications for combustion and microbial sources. *J. Geophys. Res.*, 112, 2007. doi:10.1029/2006JD007538.

M.L. Wesely. Parameterization of surface resistance to gaseous dry deposition in regional-scale numerical models. *Atmospheric Environment*, 23:1293–1304, 1989.

O. Wild, X. Zhu, and M.J.Prather. Fast-J: Accurate simulation of in- and below cloud photolysis in tropospheric chemical models. *J. of Atmos. Chem.*, 37:245–282, 2000.

P. Wind, L. Tarrasón, E. Berge, L.H. Slørdal, S. Solberg, and S.-E. Walker. Development of a modeling system able to link hemispheric- regional and local air pollution problems. MSC-W note 5/2002, The Norwegian Meteorological Institute, Oslo, Norway, 2002.